Delayed feedback control of a delay equation at Hopf bifurcation

– Dedicated to John Mallet-Paret on the occasion of his 60th birthday –

Bernold Fiedler*
Sergio Muniz Oliva**

version of January 23, 2015

*
Institut für Mathematik
Freie Universität Berlin
Arnimallee 3
14195 Berlin, Germany

**
Instituto de Matemática e Estatística
Departamento de Matemática Aplicada
Universidade de São Paulo
Rua do Matão, 1.010, Cidade Universitaria
05508-900 - São Paulo, SP - Brasil

Abstract

We embark on a case study for the scalar delay equation

$$\dot{x}(t) = \lambda f(x(t-1)) + b^{-1}(x(t-\vartheta) + x(t-\vartheta-p/2))$$

with odd nonlinearity f, real nonzero parameters λ, b, and three positive time delays 1, ϑ, $p/2$. We assume supercritical Hopf bifurcation from $x \equiv 0$ in the well-understood single-delay case $b = \infty$. Normalizing $f'(0) = 1$, branches of constant minimal period $p_k = 2\pi/\omega_k$ are known to bifurcate from eigenvalues $i\omega_k = i(k + \frac{1}{2})\pi$ at $\lambda_k = (-1)^{k+1}\omega_k$, for any nonnegative integer k. The unstable dimension is k, at the local branch k. We obtain stabilization of such branches, for arbitrarily large unstable dimension k.

For $p := p_k$ the branch k of constant period p_k persists as a solution, for any $b \neq 0$ and $\vartheta \geq 0$. Indeed the delayed feedback term controlled by b vanishes on branch k: the feedback control is noninvasive there. Following an idea of [Pyr92], we seek parameter regions $\mathcal{P}$ of controls $b \neq 0$ and delays $\vartheta \geq 0$ such that the branch k becomes stable, locally at Hopf bifurcation. We determine rigorous expansions for $\mathcal{P}$ in the limit of large k. The only two regions $\mathcal{P} = \mathcal{P}^{\pm}$ which we were able to detect, in this setting, required delays ϑ near 1, controls b near $(-1)^k \cdot 2/\omega_k$, and were of very small area of order k^{-4}. Our analysis is based on a *2-scale covering lift* for the frequencies involved.

1 Introduction and main result

In an ODE setting, *delayed feedback control* is frequently studied in systems like

$$\dot{\mathbf{x}}(t) = \mathbf{F}(\mathbf{x}(t)) + \beta(\mathbf{x}(t) - \mathbf{x}(t-\tau)) \tag{1.1}$$

with $\mathbf{x} \in \mathbb{R}^N$, smooth nonlinearities $\mathbf{F}$, and suitable $N \times N$ matrices β mediating the feedback. If the uncontrolled system $\beta = 0$ possesses a periodic orbit $\mathbf{x}_*(t)$ of (not necessarily minimal) period $p > 0$, then $\mathbf{x}_*(t)$ remains a solution of (1.1) for time delays $\tau = p$ and any control matrix β. In this sense, the delayed feedback control is noninvasive on $\mathbf{x}_*(t)$. The linearized and nonlinear stability or instability of $\mathbf{x}_*(t)$, however, may well be affected by the control term β.

The above idea was first proposed by Pyragas, see [Pyr92]. It has gained significant popularity in the applied literature since then, with currently around 3000 publications listed. See [Fie&al08] and [Pyr12] for more recent surveys. Part of this success is due to the simple implementation: let β measure some components of $\mathbf{x}(t)$, store, and feed the difference $\mathbf{x}(t) - \mathbf{x}(t-\tau)$ back into the system. Then vary the feedback gain of β, and the delay τ, until a periodic solution of (not necessarily minimal) period $p = \tau$ is found. If yes, publish. In fact, no previous knowledge of the nonlinearity $\mathbf{F}$ is required to attempt this procedure, or one of its many variants.

Mathematical results are still relatively scarce, compared to the applied significance of Pyragas control. For example it has been claimed that hyperbolic periodic orbits $\mathbf{x}_*(t)$ with *odd unstable dimension*, i.e. with Floquet multipliers $|\mu| > 1$ of odd total algebraic multiplicity, cannot be stabilized by (1.1). See for example [Nak97]. This purported *odd number limitation* has been refuted by [Fie&al07]; see also [Ju&al07, Fie&al08, Fie08] and the references there for a thorough discussion. An explicit counterexample was based on $\mathbf{x} \in \mathbb{R}^2$ and $\mathbf{F}$ in truncated Hopf normal form, a.k.a. Stuart-Landau oscillator. A careful justification of the normal form procedure, in general, was given by [BrPoSi11]. For an exciting investigation of traveling wave stabilization by noninvasive delayed spatio-temporal feedback see [PoSi07]. Systematic studies of pattern selection at symmetry breaking Hopf bifurcation have been initiated in coupled oscillator settings; see for example [NakUe98, Fie&al10, PoBrSi13, Schn13, Schn14, Cho&al14] and the references there.

One fundamental disadvantage of the Pyragas method (1.1), from a theoretical perspective, is the replacement of the ODE $\dot{\mathbf{x}} = \mathbf{F}(\mathbf{x})$ in finite-dimensional phase space $X = \mathbb{R}^N$ by the infinite-dimensional dynamical system (1.1) in a history phase space like $\mathbf{x}(t+\cdot) \in X = C^0([-\tau, 0], \mathbb{R}^N)$. On the other hand, the very existence of a periodic solution $\mathbf{x}(t)$, for vanishing control $\beta = 0$, requires $N = 2$.

In the present paper we therefore explore the Pyragas method of delayed feedback control, in a slightly modified form, for the very simplistic scalar case

$$\dot{x}(t) = \lambda f(x(t-1)) + b^{-1}(x(t-\vartheta) + x(t-\vartheta-p/2))\,. \tag{1.2}$$

We consider nonzero real parameters λ, b and positive delays. The characteristic equation for eigenvalues μ of the linearization of (1.2) at parameter λ and the trivial equilibrium $x \equiv 0$ reads

$$\mu = \lambda e^{-\mu} + b^{-1}(e^{-\vartheta\mu} + e^{-(\vartheta+p/2)\mu})\,. \tag{1.3}$$

Here we have assumed $f(0) = 0$, $f'(0) = 1$ for simplicity.

The uncontrolled limit $b = \infty$ of vanishing feedback corresponds to the scalar pure delay equation

$$\dot{x}(t) = \lambda f(x(t-1)) \tag{1.4}$$

with $|\lambda|$ normalizing the remaining delay to unity. Throughout the paper we assume $f \in C^3$ to be odd, with normalized derivative at $f(0) = 0$:

$$f(-x) = -f(x), \quad f'(0) = 1, \quad f'''(0) < 0\,. \tag{1.5}$$

See [KapYor74] for an analysis of odd periodic solutions $x_k(t)$ of constant minimal period

$$p_k := 2\pi/\omega_k, \quad \omega_k := (k + \tfrac{1}{2})\pi\,. \tag{1.6}$$

The periodic solutions originate by Hopf bifurcation from imaginary eigenvalues $\pm i\omega_k$ at $x = 0$ for parameters

$$\lambda = \lambda_k := (-1)^{k+1}\omega_k\,. \tag{1.7}$$

Here $k \in \mathbb{N}$ is any positive integer. See [Dor89] for secondary bifurcations from these primary branches. The case $\dot{x}(t) = g(x(t), x(t-1))$ of the general scalar delay equation with a single time lag has also attracted considerable attention; see for example [Wri55, BeCo63, Hale77, HaleVL93, Die&al95, Wu96, KolMysh99, Nu02] and the many references there. Most notably, Mallet-Paret has discovered a discrete Lyapunov functional for g with monotone delayed feedback, [MP88], with significant global consequences [FieMP89, Kri08, MPSe96a, MPSe96b, Wal95]. More recent developments study this scalar equation with state dependent delays, where the time delay 1 is not constant but depends on the history $x(t+\cdot)$ of the solution itself; see for example [Har&al06, MPNu96, MPNu03, MPNu11, Nu02].

But let us return to the simple setting (1.4) – (1.6) of a pure delay equation. In section 2 we will review the reduction by [KapYor74] to a planar Hamiltonian ODE system which accounts for all local Hopf bifurcations (1.7) at $\lambda = \lambda_k$, $k \in \mathbb{N}$. This is due to an *odd-symmetry*

$$x_k(t + p_k/2) = -x_k(t) \tag{1.8}$$

at half minimal period p_k, for all real t. Remarkably, global solution branches of constant minimal period p_k emanate from each $\lambda = \lambda_k$ towards λ of larger absolute value, in the soft spring case of strictly decreasing secant slopes $x \mapsto f(x)/x$,

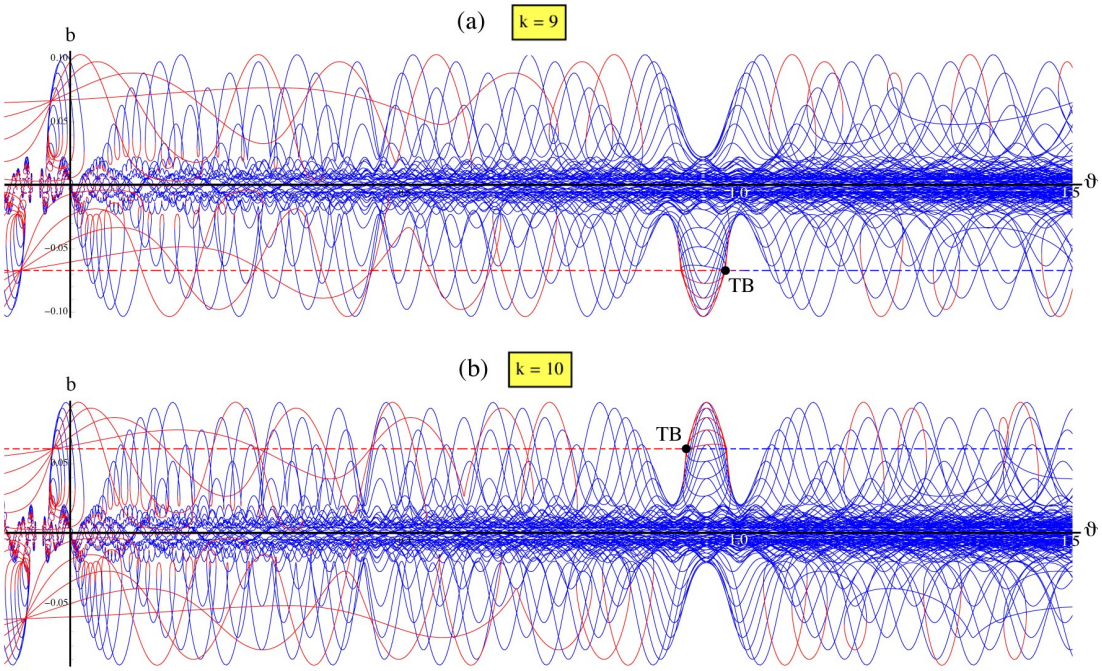

Figure 1.1: *Additional Hopf curves (colored solid), zero eigenvalue (colored dashed), and Takens-Bogdanov bifurcations (TB, black) at fixed $\lambda = \lambda_k$, for odd $k = 9$, (a) top, and even $k = 10$, (b) bottom. The Hopf curves are generated by the parameters ϑ and b of the delayed feedback terms in (1.2). Solid colors indicate orientation with respect to increasing frequency $\omega > 0$: red for increasing and blue for decreasing values of $\vartheta = \vartheta(\omega)$, respectively. In view of lemma 3.3 the more stable side is found towards smaller $|b|$, at red Hopf branches, and towards larger $|b|$, at blue branches. By lemma 3.4 the same statement holds true for the color coding of the dashed line at the zero eigenvalue.*

for $x > 0$. In particular all Hopf bifurcations are locally nondegenerate and quadratically supercritical under the sign assumption $f'''(0) < 0$ of (1.5). See fig. 3.1 for a bifurcation diagram.

At supercritical Hopf bifurcation it is easy to determine the unstable dimension E, i.e. the total algebraic multiplicity of Floquet multipliers $|\mu| > 1$, of the emanating local branch of periodic orbits. It coincides with the total algebraic multiplicity

$$E = E(\lambda_k) = k \tag{1.9}$$

of the eigenvalues with strictly positive real part for the linearization $\dot{y}(t) = \lambda_k y(t-1)$ of the pure delay equation (1.4) at the Hopf point $\lambda = \lambda_k$, $x \equiv 0$. See for example [Die&al95, Hale77, HaleVL93].

Our modified Pyragas control scheme (1.2) with $p := p_k$ is noninvasive on the global Hopf branches of constant minimal period p_k which emanate from Hopf bi-

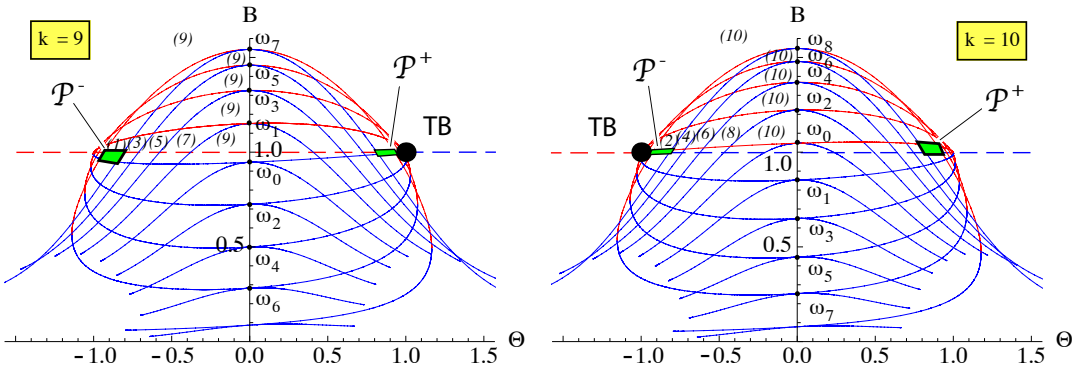

Figure 1.2: *Zoom of fig. 1.1 in scaled parameters* $\Theta = \frac{\pi}{2} + (\vartheta - 1)\,\omega_k$, $B = \frac{1}{2}(-1)^k\, b\,\omega_k$; *see also* (4.3). *Hopf curves (colored solid), zero eigenvalue (colored dashed), and the Takens-Bogdanov point (TB, black) at fixed* $\lambda = \lambda_k$, *for odd* $k = 9$, *left, and even* $k = 10$, *right. Color codings indicate change of stability as in fig. 1.1. Some resulting unstable dimensions* $E = E(\vartheta, b)$ *are indicated in parentheses as* (E). *Note* $E = 0$ *in the tiny green Pyragas regions* $\mathcal{P}^{\pm}$.

furcation at $\lambda = \lambda_k$. This is due to the odd-symmetry (1.8). In particular the global and local Hopf branches with this symmetry are preserved.

We define a *Pyragas region* $\mathcal{P}_k$ to be an open set of those real control parameters $b \neq 0$ and $\vartheta > 0$ for which the periodic solutions $x_k(t)$ emanating by local Hopf bifurcation from $\lambda = \lambda_k$, $x \equiv 0$ become linearly asymptotically stable for sufficiently small amplitudes. With this definition we can now formulate our main result. See fig. 1.1 for an illustration of Hopf curves, and fig. 1.2 for a zoom into the Pyragas regions $\mathcal{P}_k^{\pm}$, in the cases $k = 9$ and $k = 10$.

Theorem 1.1. *Consider the system* (1.2) *of delayed feedback control for the scalar pure delay equation* (1.4). *Let assumptions* (1.5) *of oddness and normalization hold for the soft spring nonlinearity* $f \in C^3$. *Then the following assertions hold for large enough* $k \geq k_0$.

There exists a Pyragas region $\mathcal{P}_k = \mathcal{P}_k^+ \cup \mathcal{P}_k^-$ *composed of two disjoint open sets* $\mathcal{P}_k^{\pm} \neq \varnothing$. *Each region* $\mathcal{P}_k^{\iota}$, $\iota = \pm$, *is bounded by the horizontal* zero line

$$b = b_k := -2/\lambda_k = (-1)^k \cdot 2/\omega_k \tag{1.10}$$

and three other analytic curves γ_k^0 *and* $\gamma_{k,\pm}^{\iota}$, *all mutually transverse. The zero line* (1.10) *indicates an additional zero eigenvalue of the linearization of* (1.2) *at* $x \equiv 0$. *The other curves indicate additional purely imaginary eigenvalues.*

Theorem 1.2. *Let the assumptions of theorem 1.1 hold and define* $\varepsilon := 1/\omega_k$. *Then an approximation of the Pyragas regions* $(\vartheta, b) \in \mathcal{P}_k^{\iota}$, $\iota = \pm$, *up to error terms of order* ε^3, *is given by two parallelograms. One exact horizontal boundary is* $b = b_k := (-1)^k\, 2\varepsilon$; *see* (1.10). *The other horizontal boundary* γ_k^0 *is approximated by*

$$b = (-1)^k\, 2\varepsilon + b_k^{\iota}\, \varepsilon^2 + \dots\,. \tag{1.11}$$

The sides $\gamma^\iota_{k,\pm}$ are given, up to order ε^3, by the parallel slanted lines through the four points at $b = b_k$,

$$\vartheta^\iota_{k,\pm} = 1 - (\tfrac{\pi}{2} - \iota\, q)\varepsilon \pm \Theta_{k+2}\,\varepsilon^2 + \dots\,, \tag{1.12}$$

with slopes σ^ι_k. Here numerical values for the offsets q, Θ_{k+2}, b^ι_k and the slopes σ^ι_k of the Pyragas parallelograms are given by

$$\begin{aligned} q = &\quad 0.88\dots\,,\\ \Theta_{k+2} = &\quad -1.73\dots\,,\\ b^\iota_k = &\quad 1.49\dots + (-1)^k\iota\cdot 1.02\dots\,,\\ \sigma^\iota_k = &\quad (-1)^{k+1}\iota\cdot 2.42\dots\,. \end{aligned} \tag{1.13}$$

Exact values are given by the expressions

$$\begin{aligned} q = &\quad \arccos\,(2/\pi)\,,\\ \Theta_{k+2} = &\quad \pi(\sqrt{(\pi/2)^2-1} - 2q)\,,\\ b^\iota_k = &\quad (\pi + 2\Phi^\iota_k)\,\cos\,\Phi^\iota_k\,,\\ \sigma^\iota_k = &\quad 2(-1)^{k+1}\iota\sqrt{(\pi/2)^2-1}\,. \end{aligned} \tag{1.14}$$

Here we have used the abbreviations

$$\Phi^\iota_k = \quad (-1)^k\iota\,\arcsin\,q\,. \tag{1.15}$$

In particular the areas $|\mathcal{P}^\pm_k|$ of the Pyragas regions are of very small order ε^4. The relative areas are approximately reciprocal,

$$\lim_{k\mapsto\infty} |\mathcal{P}^+_k|/|\mathcal{P}^-_k| = b^+_k/b^-_k = \begin{cases} 5.37\dots & \text{for even } k\,,\\ 0.19\dots & \text{for odd } k\,. \end{cases} \tag{1.16}$$

The remaining sections contribute to the proof of theorem 1.1 and the closely related ε-expansions of the Pyragas regions in theorem 1.2. We give a brief outline here. For a summary of sections 2 – 8, on a precise technical level, we also recommend the proof of theorems 1.1, 1.2 in section 9.

In section 2 we review the results by [KapYor74] on global Hopf bifurcation of the odd-symmetry periodic solutions $x_k(t)$ for the pure delay equation (1.4).

The main part of our paper is devoted to the characteristic equation (1.3) which involves three exponential terms arising from the three time delays. For a single delay see for example [BeCo63]. For two delays see [Nu78]. Section 3 addresses the characteristic equation (1.3) for the eigenvalues μ of the modified Pyragas scheme (1.2) at Hopf bifurcation $\lambda = \lambda_k$, $x \equiv 0$. We first study the appearance of an additional zero eigenvalue $\mu = 0$ at the boundary line $b = b_k = (-1)^k 2\varepsilon$ of (1.10) for the Pyragas regions $\mathcal{P}^\pm$. We also address the resulting sub- or

super-critical crossing direction of the Hopf eigenvalue $\mu = \pm i\omega_k$ as λ increases through $\lambda = \lambda_k$, in the (ϑ, b)-plane of control delay ϑ and control amplitude b. In particular, this will assure supercritical Hopf bifurcation with respect to λ for parameters (ϑ, b) fixed in the Pyragas stabilization regions $\mathcal{P}^{\pm}$. As a consequence linear asymptotic stability of the local Hopf branches bifurcating at $\lambda = \lambda_k$, $x \equiv 0$, as asserted in the theorems, will be guaranteed by

$$E_k(\vartheta, b) = 0\,. \tag{1.17}$$

in the supercritical region and off the curves of other purely imaginary or zero eigenvalues. Similarly to (1.9), here E_k indicates the total algebraic multiplicity of eigenvalues with strictly positive real part at $\lambda = \lambda_k$, $x \equiv 0$, for the linearization of the delayed feedback control scheme (1.2). This reduces the nonlinear stability question, near Hopf bifurcation, to the spectral question (1.17) for the characteristic equation.

In section 4 we rescale the parameters (ϑ, b) to (Θ, B), with ε, and introduce a *2-scale lift*

$$\Omega/\varepsilon = \omega = \Phi + (-1)^k \pi/2 \qquad (\mathrm{mod}\ 2\pi) \tag{1.18}$$

for purely imaginary Hopf eigenvalues $\pm i\omega$ of the characteristic equation (1.3). Here the rapid angle variable $-\pi/2 \le \Phi < 3\pi/2 \pmod{2\pi}$ is in S^1. The 2-scale lift allows us to view Ω and Φ as independent parameters, first, and to solve the properly rescaled characteristic equation (1.3) for (Θ, B). On the cylinder $(\Omega, \Phi) \in [0, \infty) \times S^1$, the relation (1.18) defines an ε-dependent *hashing* by slanted lines of slope $1/\varepsilon$ and horizontal distance $2\pi\varepsilon$. Therefore (1.18) also defines an ε-dependent hashing of the resulting regions

$$(\Theta, B) = (\Theta, B)\,(\Omega, \Phi) \tag{1.19}$$

in the rescaled (ϑ, b)-plane. See also (4.3), (4.6) below. The hashing provides the rather messy diagram of Hopf curves illustrated in fig. 1.1.

Section 5 obtains the Hopf curves $\gamma^{\iota}_{k,\pm}$, $\iota = \pm$ on the boundaries of the Pyragas regions $\mathcal{P}^{\iota}$ from the limiting case $\Omega = 1$. Section 6 studies the Hopf curve $(\vartheta, b) \in \gamma^0_k$ emanating from the Takens-Bogdanov point in the limit $\Omega = 0$. Section 7 addresses the characteristic equation (1.3) along the zero line (1.10), i.e. $b = b_k = (-1)^k\, 2\varepsilon$, of zero eigenvalues. In particular we determine where the remaining Hopf curves cross this line, and in which direction they cross. This keeps track of the strict unstable dimensions $E(b, \vartheta)$ along the zero line. The complementary section 8 investigates all Hopf crossings of the vertical half line $\vartheta = 1 - \frac{1}{2}\pi\,\varepsilon$, $(-1)^k(b - b_k) > 0$. In section 9, the vertical half line and the horizontal zero line will provide access to the unstable dimensions $E(\vartheta, b)$ in the Pyragas regions $\mathcal{P}^{\pm}$. See in particular lemma 9.1. We also summarize the expansions of sections 4 – 7 to prove theorem 1.2, and thereby theorem 1.1. We conclude in section 10 with a brief discussion of our results.

Acknowledgements. Most of all we are indebted to John Mallet Paret as a lasting source of friendly inspiration and encouragement. He is always ready to generously share, both, his deep intuition and perfect technique – at an equally awe-inspiring level rarely found in combination. For helpful comments, suggestions, and advice we are also indebted to Isabelle Schneider, Eckehard Schöll, and Anna Zakharova. Ulrike Geiger cheerfully converted the messy manuscript into the present form with all her expertise and singular patience. Very enjoyable mutual visits are gratefully acknowledged by both authors. The first author has been supported by CRC 910 *"Control of Self-Organizing Nonlinear Systems: Theoretical Methods and Concepts of Application"* of the Deutsche Forschungsgemeinschaft. The second author has been supported by FAPESP 2008/55516-3 and CAPES/DGU 238/11 (Brasil).

2 The pure delay equation

In this section we briefly summarize properties of odd-symmetry periodic solutions of the scalar pure delay equation

$$\dot{x}(t) = \lambda f(x(t-1))\,. \tag{2.1}$$

In other words, we assume odd nonlinearities

$$f(-x) = -f(x) \tag{2.2}$$

and seek solutions of the odd-symmetry form

$$x(t-2) = -x(t)\,. \tag{2.3}$$

See [Dor89] for a careful study of such periodic orbits, including symmetry breaking secondary bifurcations. We follow [KapYor74] to convert this problem to $\mathbb{Z}_4$-symmetric solutions $\zeta = (\xi,\, \eta)$ of the Hamiltonian ODE system

$$\begin{aligned} \dot{\xi}(t) &= \lambda\, f(\eta\,(t)) \\ \dot{\eta}(t) &= -\lambda\, f(\xi\,(t)) \end{aligned} \tag{2.4}$$

with minimal period

$$p = p_k = 2\pi/\omega_k = 4/(2k+1)\,. \tag{2.5}$$

Here $k \in \mathbb{N}_0$ is any nonnegativ integer. See lemma 2.2 and also (1.6). In lemma 2.3 we collect some standard facts on monotone dependence of minimal periods on amplitude, for the Hamiltonian system (2.4), to identify all Hopf bifurcation points $\lambda = \lambda_k = (-1)^k\omega_k$, $x \equiv 0$, of (2.1) and establish supercriticality under our standing assumptions (1.5). See also [YuGuo14] for a recent survey.

As a prelude we study the spatio-temporal symmetry of solutions $\zeta = (\xi, \eta)$ of (2.3) with minimal period $p > 0$. Let

$$\rho(\xi, \eta) := (\eta, -\xi) \tag{2.6}$$

denote standard clockwise rotation by $\pi/2$. Iteration of ρ generates the standard planar action of the cyclic group $\langle\rho\rangle = \mathbb{Z}_4$ by right rotation. See also [GoStSch88, Fie88, ChoLau00] for a general background.

Proposition 2.1.

(i) The ODE system (2.4) *is Hamiltonian with respect to*

$$H(\xi, \eta) := F(\xi) + F(\eta), \qquad F(\xi) := \int_0^\xi f(\xi')\, d\,\xi' \,, \tag{2.7}$$

and the standard symplectic structure, up to scaling factor $\lambda \neq 0$.

(ii) If f *is odd, as in* (2.2)*, then* (2.4) *is* $\mathbb{Z}_4$*-equivariant:* $\zeta(t)$ *is a solution if, and only if,* $\rho\,\zeta(t)$ *is a solution, for the rotation* ρ *given in* (2.6)*. In particular any nonstationary periodic solution* $\zeta(t)$ *of* (2.4) *which contains the origin* $\zeta = 0$ *in its interior satisfies*

$$\rho\,\zeta(t) = \zeta(t \pm p/4)\,. \tag{2.8}$$

Here p *denotes the minimal period of* $\zeta(t)$*.*

(iii) Assume f *is odd and also satisfies the sign constraint*

$$x f(x) > 0 \tag{2.9}$$

for all $x > 0$*. Then any nonzero solution* $\zeta(t)$ *of* (2.4) *is nonstationary periodic and contains the origin in the interior. Moreover* $\zeta(t)$ *satisfies*

$$\rho\,\zeta(t) = \begin{cases} \zeta(t - p/4) & \text{for} \quad \lambda < 0\,, \\ \zeta(t - 3p/4) & \text{for} \quad \lambda > 0\,. \end{cases} \tag{2.10}$$

Proof. Claim (i) is obvious. Equivariance claim (ii) is straightforward:

$$\begin{aligned} \tfrac{d}{dt}\rho\,\zeta = \rho\,\dot\zeta = (\dot\eta, -\dot\xi) = \big(-\lambda f(\xi), -\lambda f(\eta)\big) = \\ = \lambda\big(f(-\xi), -f(\eta)\big) = \big(\lambda f\big((\rho\,\zeta)_2\big), -\lambda f((\rho\,\zeta)_1)\big)\,, \end{aligned} \tag{2.11}$$

i.e. $\rho\,\zeta$ solves (2.4) if, and only if, ζ does. Here we used oddness (2.2) of f in the fourth equality.

To prove symmetry claim (2.8) first observe that the periodic orbits ζ and $\rho\,\zeta$ must intersect and hence coincide. Therefore $\mathbb{Z}_4$ is a spatio-temporal symmetry of ζ:

$$\rho\,\zeta(t) = \zeta(t + t_0) \neq 0 \tag{2.12}$$

for some fixed t_0 and all real t. Since 0 is the only fixed point of any non-identity element of $\mathbb{Z}_4$, and $\rho^4 = \mathrm{id}$, this implies $t_0 = \pm p/4$. This proves claim (ii).

To prove claim (iii), first observe that the primitive $\mathbf{F}(\xi)$ of f is strictly increasing with $|\xi|$, by positivity assumption (2.9). In particular any level set of H is bounded. Moreover $0 = \min H$ is the only critical value of H, and has the unique critical point $\zeta = 0$. All other nonempty level sets of H are regular Jordan curves with $\zeta = 0$ in the interior. In particular any nontrivial solution $\zeta(t) \not\equiv 0$ is periodic around $(\xi, \eta) = (0, 0)$.

The remaining symmetry claim (2.10) follows from claim (ii) and positivity assumption (2.9). Let $\eta(0) > 0 = \xi(0)$ denote an intersection point of $\zeta(t)$ with the positive η-axis and assume $\lambda > 0$. Then (2.9) implies $\dot\xi(0) = \lambda f(\eta(0)) > 0$. Hence $\zeta(t)$ crosses the positive η-axis clockwise. Equivariance implies clockwise crossing of all other half axes, successively at times $p/4$, $p/2$, $3p/4$. In particular $\rho\,\zeta(t) = \zeta(t + p/4) = \zeta(t - 3p/4)$, initially at $t = 0$, and hence for all real t. Since $\lambda \mapsto -\lambda$ just reverses the time direction in ODE (2.4), this proves claim (2.10) of (iii), and the proposition. ⋈

Lemma 2.2. *[KapYor74] Assume oddness* (2.2) *and positivity* (2.9) *of the nonlinearity f. Consider the transformation*

$$\xi(t) = x(t), \quad \eta(t) = x(t-1)\,. \tag{2.13}$$

Then $x(t)$ is a nontrivial periodic solution of the pure delay equation (2.1) *with odd-symmetry* (2.3)*, for all real t if, and only if, $\zeta(t) := (\xi(t), \eta(t))$ satisfies the following. The Hamiltonian ODE* (2.4) *is solved by $\zeta(t) \not\equiv 0$ with minimal period*

$$p = p_k = 4/(2k+1)\,, \tag{2.14}$$

for some $k \in \mathbb{N}_0$. See (1.6)*. More precisely k is odd, for $\lambda > 0$, and even, for $\lambda < 0$.*

Proof. Let $x(t) \not\equiv 0$ solve (2.1) with odd-symmetry (2.3). Then (2.13) implies

$$\dot\xi(t) = \dot x(t) = \lambda f\big(x(t-1)\big) = \lambda f\big(\eta(t)\big)\,. \tag{2.15}$$

Because f is odd, (2.1), (2.3) and (2.13) also imply

$$\begin{aligned} \dot\eta(t) = \dot x(t-1) = \lambda f\big(x(t-2)\big) = \lambda f\big(-x(t)\big) = \\ = -\lambda f\big(x(t)\big) = -\lambda f\big(\xi(t)\big)\,. \end{aligned} \tag{2.16}$$

Therefore $\zeta = (\xi, \eta)$ solves the ODE (2.4).

By proposition 2.1, the solution $\zeta = \zeta(t) \not\equiv 0$ is periodic with minimal period $p > 0$ and satisfies (2.10). By (2.3) we have $p = 4/m$ for some positive integer

m. Consider $\lambda < 0$ first. Then the first components of (2.10), (2.6) and the transformation (2.13) successively imply

$$\xi(t - p/4) = \big(\rho\,\zeta(t)\big)_1 = \eta(t) = x(t-1) = \xi(t - mp/4)\,, \tag{2.17}$$

Therefore (2.13) also implies $\zeta(t - p/4) = \zeta(t - mp/4)$. Because $p > 0$ is the minimal period of ζ we conclude $m = 2k+1$ for some even $k \in \mathbb{N}_0$. The argument for $\lambda > 0$ is completely analogous and is omitted. This proves the only-if part of the lemma.

To prove the if-part, let $\zeta(t) = (\xi(t),\, \eta(t)) \not\equiv 0$ solve the Hamiltonian ODE (2.4) with minimal period $p = p_k = 4/(2k+1)$ as in (2.14). Again we only consider the case $\lambda < 0$ of even $k \geq 0$. We first show that $x(t) := \xi(t)$ satisfies the pure delay equation (2.1). By ODE (2.4) this is equivalent to showing

$$\eta(t) = \xi(t-1)\,. \tag{2.18}$$

To prove claim (2.18) we substitute $1 = (2k+1)\,p/4$ to obtain

$$\xi(t-1) = \xi\big(t - (2k+1)\,p/4\big) = \xi(t - p/4) = \big(\rho\,\zeta(t)\big)_1 = \eta(t)\,, \tag{2.19}$$

as claimed in (2.18). Similarly

$$\xi(t-2) = \xi(t - 2p/4) = \big(\rho^2\,\zeta(t)\big)_1 = -\xi(t) \tag{2.20}$$

implies odd-symmetry (2.3) of $x(t) = \xi(t)$, and the lemma is proved. ⋈

For *soft spring nonlinearities* f it is assumed that

$$x \mapsto f(x)/x > 0 \tag{2.21}$$

decreases strictly with increasing $|x| > 0$. For pendulum equations $\ddot{\xi} + \lambda^2 f(\xi) = 0$ it is well-known that the minimal period p^λ then increases strictly with amplitude; see e.g. [BiRo62, Scha90]. Here we use superscripts λ to emphasize dependence on the scaling parameter $\lambda \neq 0$. The same arguments apply to solutions $\zeta^\lambda(t)$ of (2.4) and their minimal periods $p^\lambda(a) > 0$. Amplitude $\sqrt{H}$ can be measured by the value of the Hamiltonian $H = H(\zeta^\lambda)$, for example; see proposition 2.1(i). A global bifurcation diagram for the odd-symmetry solutions $x^\lambda(t)$ of (2.1) is easily derived.

Lemma 2.3. *Consider odd nonlinearities f which satisfy* (2.21)*. Then non-trivial odd-symmetry solutions $x^\lambda(t)$ of the pure delay equation* (2.1), (2.2) *with amplitude $\sqrt{H}$ occur if, and only if,*

$$\lambda = \lambda_k(H) = (-1)^{k+1}(2k+1)\,p\,(H)/4\,, \tag{2.22}$$

for any $k \in \mathbb{N}_0$. Here $p\,(H)$ indicates the minimal period of the solution $\zeta(t) = (\xi(t),\, \eta(t))$ of the ODE Hamiltonian system (2.4)*, for $\lambda = 1$ and $H = H(\zeta)$. The*

solution $x^\lambda(t)$ *is given by* $\xi^\lambda(t) = \xi(\lambda\, t)$ *and possesses constant minimal period* $p_k = p\,(H)/|\lambda| = 4/(2k+1)$.

In particular, local Hopf bifurcation of (2.1), (2.2) *with* $f'(0) = 1$ *only occurs at*

$$\lambda = \lambda_k(0) = (-1)^{k+1}\,\omega_k\,, \tag{2.23}$$

as mentioned in (1.7). *All bifurcating periodic solutions* $x^\lambda(t)$ *satisfy odd-symmetry property* (2.3), *locally. Under assumption* (1.5) *all Hopf bifurcations are supercritical.*

Proof. By lemma 2.2, any nontrivial odd-symmetry solution $x^\lambda(t)$ of (2.1), (2.2) arises as the first component $x^\lambda(t) = \xi^\lambda(t)$ of a solution $\zeta^\lambda(t)$ of the Hamiltonian ODE (2.4) with constant minimal period

$$p^\lambda = p_k^\lambda = 4/(2k+1) > 0\,, \tag{2.24}$$

for some $k \in \mathbb{N}_0$ of the appropriate parity; see (2.14). Rescaling time in (2.4) we obtain

$$\begin{aligned} \zeta^\lambda(t) &= \zeta^1(\lambda\, t)\,, \\ p^\lambda &= p^1/|\lambda| \end{aligned} \tag{2.25}$$

with the same Hamiltonian $H(\zeta^\lambda) = H(\zeta^1) = H$. Dropping the superscript 1, for $\lambda = 1$, and combining (2.25), (2.24) we obtain the global bifurcation diagram

$$\lambda = (-1)^{k+1}|\lambda| = (-1)^{k+1}\,p/p^\lambda = (-1)^{k+1}(2k+1)\,p\,(H)/4\,, \tag{2.26}$$

as claimed in (2.22).

To prove (2.23) we observe that $f'(0) = 1$ implies $p\,(H) \to 2\pi$ for $H \to 0$. Since $\omega_k = (k + 1/2)\pi$ by (1.6) this proves (2.23) alias (1.7); see also the characteristic equation (1.3) at $b = \infty$. In lemma 3.1 below we will show that the simple eigenvalues $\mu = \pm i\,\omega_k$ of the characteristic equation (1.3) for $b = \infty$ are the only purely imaginary eigenvalues at $\lambda = \lambda_k(0)$, and cross the imaginary axis from left to right transversely, as $|\lambda|$ increases through $\lambda = \lambda_k(0)$. Uniqueness of local Hopf branches therefore implies odd-symmetry of the periodic orbits $x(t)$, for odd nonlinearities f.

Monotonicity of the time-map $H \mapsto p^1(H)$ implies bifurcation to larger values of $|\lambda|$ from the Hopf bifurcation at $\lambda = \lambda_k(0)$, $x \equiv 0$, for soft spring nonlinearities f. The assumptions $f'(0) = 1$, $f'''(0) < 0$ imply the soft spring property (2.21) to hold locally, by Taylor expansion of odd f. Perturbations of $f'''(0)$ show that the Hopf bifurcation is in fact quadratically nondegenerate. Therefore the Hopf bifurcations at $\lambda = \lambda_k(0)$ are supercritical. This proves the present lemma once the spectral analysis is completed, in lemma 3.1. $\bowtie$

3 The characteristic equation

We linearize the delay equation (1.2) at $x \equiv 0$ and seek exponential solutions $\exp(\mu\, t)$ to obtain the characteristic equation (1.3) for $\mu \in \mathbb{C}$. For purely imaginary $\mu = i\,\omega$, $\omega \geq 0$, we obtain

$$i\,\omega = \lambda e^{-i\,\omega} + 2b^{-1}\cos\left(p\,\omega/4\right) e^{-i\,\omega(\vartheta+p/4)}\,. \tag{3.1}$$

Here we have used the normalization $f'(0) = 1$ of (1.5). A trivial solution at the Hopf bifurcation points $\lambda = \lambda_k$ is given by

$$\lambda = \lambda_k = (-1)^{k+1}\omega_k, \quad \omega = \omega_k = (k + \tfrac{1}{2})\pi, \quad p = p_k = 2\pi/\omega_k \tag{3.2}$$

for all real values of b and ϑ, of course. In lemma 3.1 we study the transverse crossing of $\mu = \pm i\,\omega_k$ through the imaginary axis, for the uncontrolled case $b = \infty$, as λ increases through λ_k. In lemma 3.2 we show how the crossing direction of μ at $\lambda = \lambda_k$ depends on b, ϑ. Pinning $\lambda = \lambda_k$ and $p = p_k$, in lemma 3.3, we begin to study the resulting additional Hopf curves

$$(\vartheta,\, b) = \big(\vartheta(\omega),\, b(\omega)\big)\,, \tag{3.3}$$

oriented along increasing frequency $\omega > 0$. This is based on the pinned characteristic equation (3.15). In particular we discuss the strict unstable dimensions

$$E = E(\vartheta,\, b) \tag{3.4}$$

to either side of any Hopf curve; see (3.18). The eigenvalue zero and the Takens-Bogdanov point $\omega \to 0$ are addressed in lemma 3.4.

Lemma 3.1. *Let $b = \infty$. Then purely imaginary eigenvalues occur if, and only if, $\lambda = \lambda_k$ for some $k \in \mathbb{N}_0$. The simple eigenvalues $\mu = \mu(\lambda)$ with $\mu(\lambda_k) = \pm i\,\omega_k$ satisfy*

$$\operatorname{sign} \operatorname{Re} \mu'(\lambda_k) = \operatorname{sign} \lambda_k\,. \tag{3.5}$$

At $\lambda = \lambda_k$, this is the only pair of purely imaginary eigenvalues. Moreover

$$E = E(\lambda) = k \tag{3.6}$$

holds for the total strict unstable dimension E of $x \equiv 0$ at any value λ between λ_{k-2} and λ_k, including $\lambda = \lambda_k$.

This lemma shows that the local Hopf bifurcations of the pure delay equation (2.1) are indeed supercritical; see also lemma 2.3. The odd-symmetry (2.3) of the periodic solution is inherited from the linearization because f is odd. Standard exchange of stability in the two dimensional center manifolds establishes the strong unstable dimension k of the bifurcating local branches [HaleVL93, Die&al95]. See fig. 3.1 for illustration. By noninvasivity of Pyragas control, these bifurcations remain unaffected by $(b,\, \vartheta)$ for $p = p_k$ – but unstable dimensions may change.

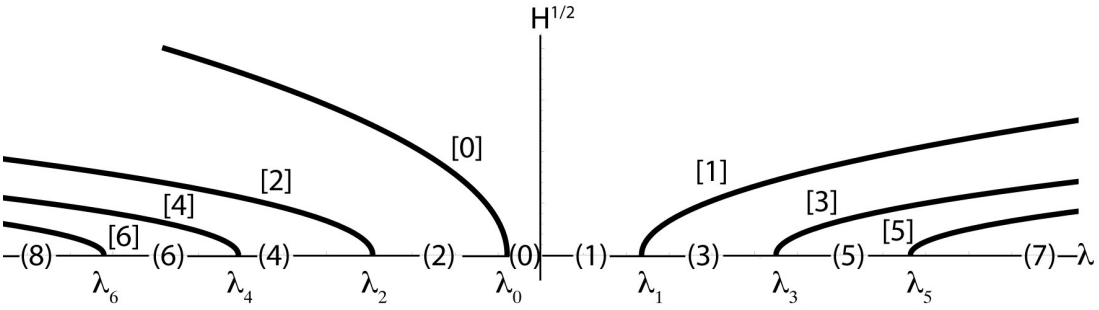

Figure 3.1: *Supercritical Hopf bifurcations at $\lambda = \lambda_k$. Note the strict unstable dimensions $E(\lambda_k) = k$ of the trivial equilibrium, in parentheses (k), and the inherited unstable dimensions $[k]$ of the local branches of bifurcating periodic orbits with constant minimal period $p_k = 4/(2k+1)$. Amplitude is measured by the constant Hamiltonian $H^{1/2}$ of (2.7). See lemmas 2.3 and 3.1.*

Proof. For $b = \infty$, the characteristic equation (1.3) simplifies to

$$\chi(\lambda,\, \mu) := \mu - \lambda\, e^{-\mu} = 0\,. \tag{3.7}$$

Decomposing into real and imaginary parts, we obtain nonzero purely imaginary eigenvalues $\mu = \pm i\,\omega$ if, and only if, $\lambda = \lambda_k$, $\omega = \omega_k$, $k \in \mathbb{N}_0$. Partial differentiation of $\chi(\lambda,\, \mu)$ at $\lambda = \lambda_k$, $\mu = i\,\omega$ yields

$$\begin{aligned} \partial_\mu \chi &= 1 + \lambda_k \exp(-i\,\omega_k) = 1 + i\,\omega_k \neq 0\,, \\ \partial_\lambda \chi &= -\exp(-i\,\omega_k) = (-1)^k i\,. \end{aligned} \tag{3.8}$$

This shows simplicity of $\pm i\,\omega_k$ and absence of other purely imaginary eigenvalues at $\lambda = \lambda_k$. Furthermore

$$\begin{aligned} \operatorname{sign} \operatorname{Re} \mu'(\lambda_k) &= \operatorname{sign} \operatorname{Re} \left(-\partial_\lambda \chi / \partial_\mu \chi\right) = \operatorname{sign}\big((-1)^{k+1} \operatorname{Im} \partial_\mu \chi\big) = \\ &= (-1)^{k+1} = \operatorname{sign} \lambda_k\,, \end{aligned} \tag{3.9}$$

by implicit differentiation of $\chi = 0$. This proves claim (3.5).

To determine $E(\lambda)$ we consider the simple real eigenvalue $\mu = 0$ at $\lambda = 0$. Real continuation $\mu(\lambda)$ yields $\mu'(0) = 1$ and hence $E(\lambda) = 0$ for $\lambda < 0$ and $E(\lambda) = 1$ for $\lambda > 0$ near 0. At $\lambda = \lambda_k$, crossing (3.5) implies that $E(\lambda)$ increases by two, alternatingly at negative and positive $\lambda = \lambda_k$ depending on the even and odd parity of k, in the direction of increasing $|\lambda|$. This proves claim (3.6), and the lemma. ⋈

Lemma 3.2. *In the notation of lemma 3.1 but now for arbitrary real control parameters $b \neq 0$, $\vartheta \geq 0$ we obtain transverse crossing*

$$\operatorname{sign} \operatorname{Re} \mu'(\lambda_k) = (-1)^{k+1} \operatorname{sign} b \cdot \operatorname{sign}\big(b + \pi \omega_k^{-2} \sin(\omega_k \vartheta)\big) \tag{3.10}$$

for nonzero right-hand sides.

Proof. Analogously to (3.7), (3.8) we let $\chi = \chi(\lambda, \mu)$ denote the difference between the left-hand and right-hand sides of the full characteristic equation (1.3). At $\lambda = \lambda_k$, $\mu = i\,\omega_k$, $p = p_k = 2\pi/\omega_k$, the partial derivatives are

$$\partial_\mu \chi = 1 + i\,\omega_k - \frac{p_k}{2b}\, e^{-i\,\omega_k\,\vartheta}\,, \tag{3.11}$$

and $\partial_\lambda \chi = (-1)^k\, i$ as before. Following (3.9) we obtain

$$\begin{aligned} \operatorname{sign} \operatorname{Re} \mu'(\lambda_k) &= \operatorname{sign}\big((-1)^{k+1} \operatorname{Im} \partial_\mu \chi\big) = \\ &= (-1)^{k+1} \operatorname{sign}\Big(\omega_k + \frac{p_k}{2b} \sin(\omega_k\,\vartheta)\Big)\,. \end{aligned} \tag{3.12}$$

This proves (3.10). ⋈

For small $\varepsilon = 1/\omega_k$, our theorems 1.1 and 1.2 claim Pyragas regions with $b = (-1)^{k+1} \cdot 2\varepsilon + \ldots$. Since (3.10) shows that the direction $\operatorname{Re} \mu'(\lambda_k)$ switches at b of order ε^2, only, we may safely ignore this switching henceforth. In other words we may safely assume supercritical switching

$$\operatorname{sign} \operatorname{Re} \mu'(\lambda) = (-1)^{k+1}\,, \tag{3.13}$$

henceforth. In particular we achieve Pyragas stabilization of the supercritical Hopf branch bifurcating at $\lambda = \lambda_k$, $x \equiv 0$, if, and only if, we show

$$E(\vartheta,\, b) = 0 \tag{3.14}$$

for the total unstable dimension $E = E(\vartheta, b)$ of (1.3) at fixed $\lambda = \lambda_k = (-1)^{k+1}\,\omega_k$, $p = p_k = 2\pi/\omega_k$ as in (3.2). This assumes absence of further purely imaginary eigenvalues, of course. For this reason we now fix $\lambda = \lambda_k$, $p = p_k$ and study the *pinned characteristic equation*

$$0 = \chi_k(\mu,\, \vartheta,\, b) := \mu - \lambda_k\, e^{-\mu} - b^{-1}\, e^{-\vartheta\,\mu}(1 + e - p_k\,\mu/2)\,. \tag{3.15}$$

We first discuss the additional *Hopf curves* $0 < \omega \mapsto \big(\vartheta(\omega),\, b(\omega)\big)$ of (3.3), which result from the pinned characteristic equation

$$0 = \chi_k(i\,\omega,\, \vartheta,\, b) = i\,\omega - \lambda_k\, e^{-i\,\omega} - 2b^{-1}\, e^{-(\vartheta + p_k/4)\,i\,\omega} \cos\,(p_k\,\omega/4)\,. \tag{3.16}$$

The next two lemmas relate, in particular, the red/blue color-coding of figs. 1.1, 1.2, 4.1 to the change of stability by decreasing $|b|$; see (3.18) and (3.23).

Lemma 3.3. *Decomposing χ_k into real and imaginary parts we obtain the sign of the Jacobian determinant*

$$\operatorname{sign} \det \partial_{(\vartheta,\, b)} \chi_k(i\,\omega,\, \vartheta,\, b) = -\operatorname{sign} b\,, \tag{3.17}$$

at $\chi_k = 0$ and $0 < \omega \neq \omega_k$. In particular the Hopf curves (3.3) are well-defined. For $b < 0$ and nonvanishing tangents, the total unstable dimension $E(\vartheta, b)$ to the right of the oriented Hopf curve exceeds the left value by 2. For $b > 0$ this jump is reversed. In symbols

$$\big[E(\vartheta,\, b)\big]^{\text{right}}_{\text{left}} = -2 \operatorname{sign} b\,, \tag{3.18}$$

along any Hopf curve oriented by increasing frequency $\omega > 0$.

Proof. Consider $\omega > 0$. To prove (3.17) we can ignore the common complex prefactor to the columns of the Jacobian $\partial_{(\vartheta,\, b)}\chi_k$ which equals $i\,\omega - \lambda_k \exp(-i\,\omega)$ at $\mu = i\,\omega$ and $\chi_k = 0$. Note that the prefactor vanishes at $\omega = \omega_k$, only; see (3.7). Therefore

$$\operatorname{sign}\det \partial_{(\vartheta,\, b)}\chi_k(i\,\omega, \vartheta,\, b) = \operatorname{sign}\det \begin{pmatrix} 0 & -1/b \\ -\omega & 0 \end{pmatrix}, \tag{3.19}$$

proving (3.17).

To prove (3.18) we observe that $\partial_{(\vartheta,\, b)}\chi$ preserves orientation, for $b < 0$. Since χ is complex analytic in μ, we also have orientation preservation by $\det \partial_\mu \chi > 0$, at nonvanishing tangents to the Hopf curves (3.3). Therefore the implicit map

$$\mu \mapsto \big(\vartheta(\mu),\, b(\mu)\big) \tag{3.20}$$

and its local inverse both preserve orientation. Since E jumps by $+2$, trivially, when μ crosses the positively orientated imaginary axis left to right, the same holds true when $(\vartheta,\, b)$ crosses any Hopf curve left to right, for $b < 0$. For $b > 0$ the sides in $(\vartheta,\, b)$ are reversed, because $\det \partial_{(\vartheta,\, b)}\chi < 0$ there. This proves (3.18) and the lemma. ⋈

Lemma 3.4. *The pinned characteristic equation $\chi_k(\mu,\, \vartheta,\, b) = 0$ of (3.15) admits an eigenvalue $\mu = 0$ if, and only if,*

$$b = b_{\mathrm{TB}} := (-1)^k \cdot 2/\omega_k\,. \tag{3.21}$$

This zero $\mu = 0$ of χ_k is algebraically simple for all values of ϑ, except at

$$\vartheta = \vartheta_{\mathrm{TB}} := 1 + \big(-\tfrac{\pi}{2} + (-1)^{k+1}\big)/\omega_k \tag{3.22}$$

where an algebraically double zero $\mu = 0$ of χ_k occurs. We call $(\vartheta_{\mathrm{TB}},\, b_{\mathrm{TB}})$ the Takens-Bogdanov point *of χ_k. For $\vartheta \neq \vartheta_{\mathrm{TB}}$, the real continuation $\mu = \mu(\vartheta,\, b)$ of the simple zero $\mu(\vartheta,\, b_{\mathrm{TB}}) = 0$ possesses nonvanishing partial derivative*

$$\operatorname{sign} \partial_b\, \mu\,(\vartheta,\, b_{\mathrm{TB}}) = (-1)^k \operatorname{sign}\,(\vartheta_{\mathrm{TB}} - \vartheta)\,. \tag{3.23}$$

Proof. Taylor expansion of the characteristic function $\chi_k(\mu,\, \vartheta,\, b)$ in (3.15) with respect to μ, at $\mu = 0$, yields

$$\chi_k(\mu,\, \vartheta,\, b) = \chi_0(\vartheta,\, b) + \chi_1(\vartheta,\, b)\mu + \chi_2(\vartheta,\, b)\mu^2 + \dots\,, \tag{3.24}$$

where we have suppressed the index k in the coefficients. Explicitly, the coefficients are

$$\begin{aligned} \chi_0(\vartheta,\, b) &= (-1)^k\omega_k - 2/b\,; \\ \chi_1(\vartheta,\, b) &= (-1)^{k+1}\omega_k + 1 + (2\vartheta + \pi/\omega_k)/b\,; \\ \chi_2(\vartheta,\, b) &= (-1)^k\omega_k/2 - (\vartheta^2 + \pi\,\vartheta/\omega_k + \tfrac{1}{2}\pi^2/\omega_k^2)/b\,. \end{aligned} \tag{3.25}$$

From $\chi_0 = 0$ we obtain the zero line (3.21) of b. Setting $\chi_1 = 0$, in addition, we obtain the Takens-Bogdanov value (3.22) of ϑ. Observing $\chi_2(\vartheta_{\mathrm{TB}},\, b_{\mathrm{TB}}) \neq 0$ shows algebraic multiplicity two of $\mu = 0$, at $b = B_{\mathrm{TB}}$, $\vartheta = \vartheta_{\mathrm{TB}}$. Implicit differentiation with respect to b shows (3.23) and completes the proof of the lemma. ⋈

4 The 2-scale lift

In (4.2) below we introduce the 2-scale lift $\omega \mapsto (\Omega,\, \Phi)$ for the frequency parameter ω of the Hopf curves. We begin with a suitable scaling to new variables

$$(\omega,\, \vartheta,\, b) \mapsto (\Omega,\, \Phi,\, \Theta,\, B), \qquad \varepsilon := 1/\omega_k\,. \tag{4.1}$$

Here $\varepsilon > 0$ denotes a fixed small parameter corresponding to large k. Slow Ω and rapid Φ correspond to the same variable ω, and constitute the 2-scale lift announced in (1.18). We rewrite the pinned characteristic equation (3.16) for the Hopf curves in terms of the scaled variables $(\Omega,\, \Phi,\, \Theta,\, B)$; see (4.5). In lemma 4.1 we derive explicit expressions for the solutions

$$(\Theta,\, B) = \big(\Theta\,(\Omega,\, \Phi),\, B\,(\Omega,\, \Phi)\big) \tag{4.2}$$

of the rescaled pinned equations, by mere trigonometry.

For the remaining sections 4 to 7 it is useful to introduce suitable *scaled variables* Θ and B by

$$\begin{aligned} \vartheta &= 1 + (-\tfrac{\pi}{2} + \Theta)\,\varepsilon\,, & \Theta &:= (\vartheta - 1)\,\varepsilon^{-1} + \tfrac{\pi}{2}\,, \\ b &= (-1)^k \cdot 2\,B\,\varepsilon\,, & B &:= \tfrac{1}{2}(-1)^k\, b\,\varepsilon^{-1}\,. \end{aligned} \tag{4.3}$$

Here and below we abbreviate $\varepsilon := 1/\omega_k$ and suppress k. See fig. 4.1 for the Takens-Bogdanov zooms of fig. 1.2 with increasing values of k.

For the single Hopf frequency $\mu = i\,\omega$ we introduce the 2-*scale lift* to the two new variables Ω, Φ by

$$\begin{aligned} \Omega &:= \omega\,\varepsilon\,, \\ \Phi &:= \omega + (-1)^{k+1}\pi/2\,. \end{aligned} \tag{4.4}$$

Here $-\pi/2 \le \Phi < 3\pi/2$ is taken $\bmod 2\pi$. In terms of the scaled variables ε, Ω, Φ, Θ, B we can rewrite the characteristic equation $\chi_k(i\,\omega,\, \vartheta,\, b) = 0$ of (3.16), as

$$0 = \chi(\Omega,\, \Phi,\, \Theta,\, B) := 1 - \Omega e^{i\,\Phi} - B^{-1}\cos(\tfrac{\pi}{2}\,\Omega)\,e^{-i\,\Omega\Theta}\,. \tag{4.5}$$

Here we have replaced λ_k, p_k in (3.15) by ω_k, via (3.2), and then $1/\omega_k$ by ε. Finally all remaining ε-terms were eliminated by the 2-scale lift (4.4). The advantage is clear: the solution set of (4.5) is independent of ε. The Hopf curves, i.e. the solutions of the equation $\chi_k(i\,\omega,\, \vartheta,\, b) = 0$ for the Hopf curve $(\vartheta,\, b) = (\vartheta,\, b)(\omega)$ appear as a *hashing*

$$\Phi = \Omega\,\varepsilon^{-1} + (-1)^{k+1}\pi/2 \pmod{2\pi} \tag{4.6}$$

in the solution map (4.2), via the scaling (4.3). See also (1.18).

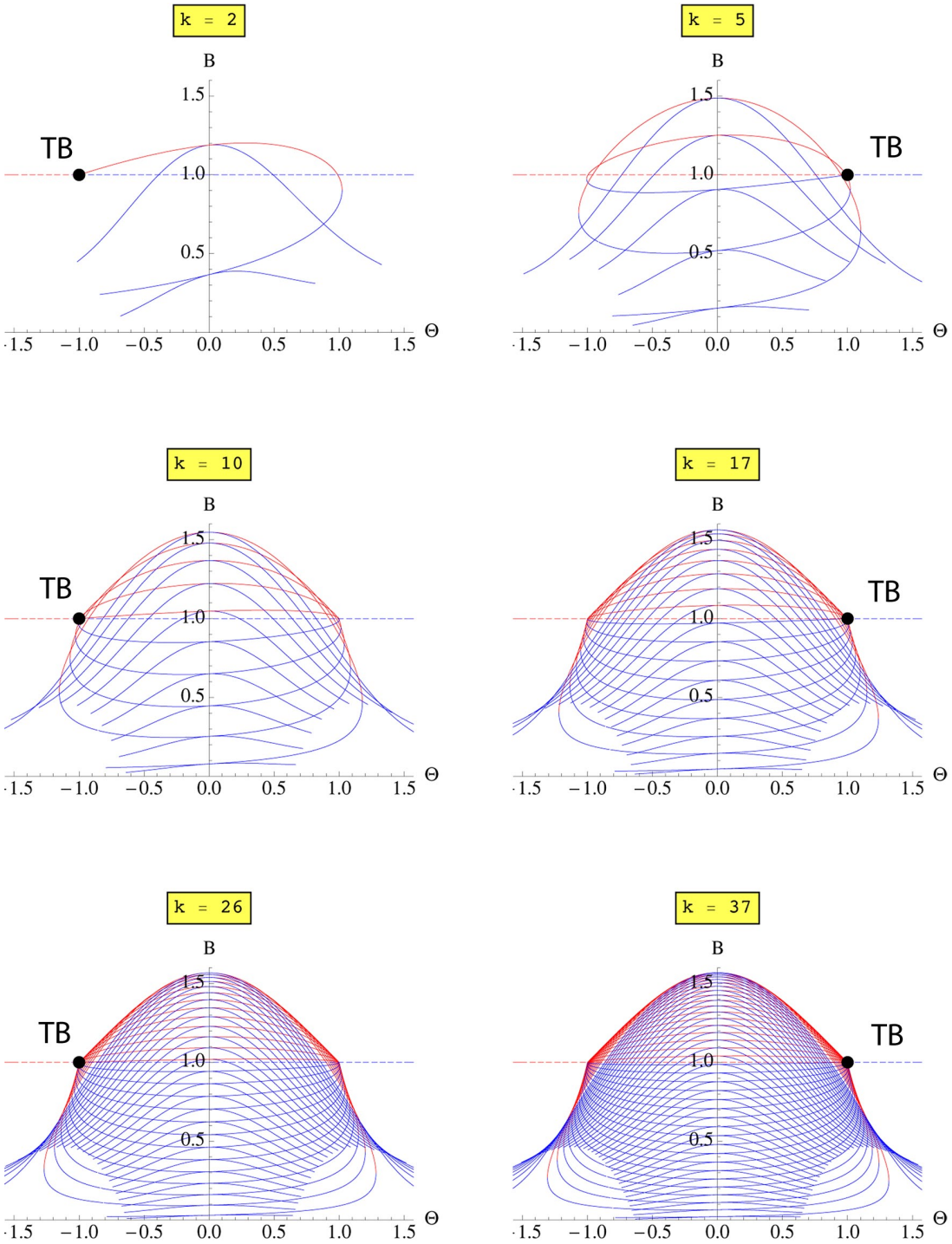

Figure 4.1: *Zooms of the Takens-Bogdanov spirals of fig. 1.2 in the scaled coordinates* (Θ, B) *of* (4.3)*, for increasing hashing values* k*. Note the Takens-Bogdanov points at* $\Theta = (-1)^{k+1}$*,* $B = 1$*. Color codings are as in figs. 1.1, 1.2.*

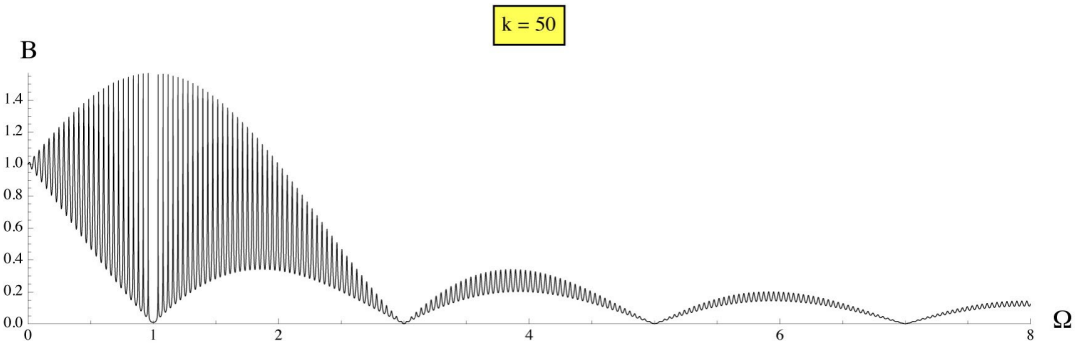

Figure 4.2: *Domain of definition* (4.8)*, hashed by* $k = 50$*, for the explicit analytic solution* (4.7) *of the scaled characteristic equation* (4.5)*. Note the resonance gap at* $\Omega = 1$*.*

Lemma 4.1. *Explicit solutions of the scaled* ε*-independent characteristic equation* $\chi(\Omega, \Phi, \Theta, B) = 0$ *in* (4.5) *are given by the conjugate branches for* (Φ, Θ) *in terms of* (Ω, B) *as*

$$\begin{aligned} \Phi &= \pm 2 \arctan \left((1-\Omega) \sqrt{\frac{\cos^2(\tfrac{\pi}{2}\,\Omega)/((\Omega-1)B)^2 - 1}{(\Omega+1)^2 - \cos^2(\tfrac{\pi}{2}\,\Omega)/B^2}} \right) \\ \Theta &= \pm 2\,\Omega^{-1} \arctan \sqrt{\frac{\Omega^2 - (1 - B^{-1}\cos\,\tfrac{\pi}{2}\,\Omega)^2}{(1 + B^{-1}\cos\,\tfrac{\pi}{2}\,\Omega)^2 - \Omega^2}}\,. \end{aligned} \tag{4.7}$$

Of course arctan *is understood here to admit addition of any integer multiple* $j\,\pi$ *of* π*. The branches are analytic for* (Ω, B) *in the domain of positive* Ω *and* B *such that*

$$|\cos\,\tfrac{\pi}{2}\,\Omega|/(1+\Omega) < B < |\cos\,\tfrac{\pi}{2}\,\Omega|/|\Omega - 1|\,. \tag{4.8}$$

Explicit solutions for (Θ, B) *in terms of* (Ω, Φ) *take the polar coordinate form*

$$B\,e^{i\,\Omega\Theta} = \cos\,(\tfrac{\pi}{2}\,\Omega)/(1 - \Omega\,e^{i\,\Phi})\,. \tag{4.9}$$

For strictly positive values of Ω *and* B*, the only relevant singularity of* (4.9) *where analyticity may fail is at* $\Omega = 1$ *and* $\Phi = 0$*.*

Proof. By complex conjugation any real vector $(\Omega, \Phi, \Theta, B)$ solves (4.5) if, and only if, $(\Omega, -\Phi, -\Theta, B)$ does. This accounts for the $\pm$ branches.

The explicit expressions (4.7) follow by standard trigonometry in the triangle **0A1** of fig. 4.3. Indeed, the three sides of length 1, Ω, $B^{-1}\cos\,(\frac{\pi}{2}\,\Omega)$ determine the angles Φ and $\Omega\Theta, \mathrm{mod}\,2\pi$. The domain (4.8) is the region where two circles intersect: the circle of radius $B^{-1}|\cos\,\Theta|$ around 1 and the circle of radius Ω around 1. Indeed the boundaries of the domain (4.8) are characterized by tangencies of the circles, and hence by $\Theta = 0$.

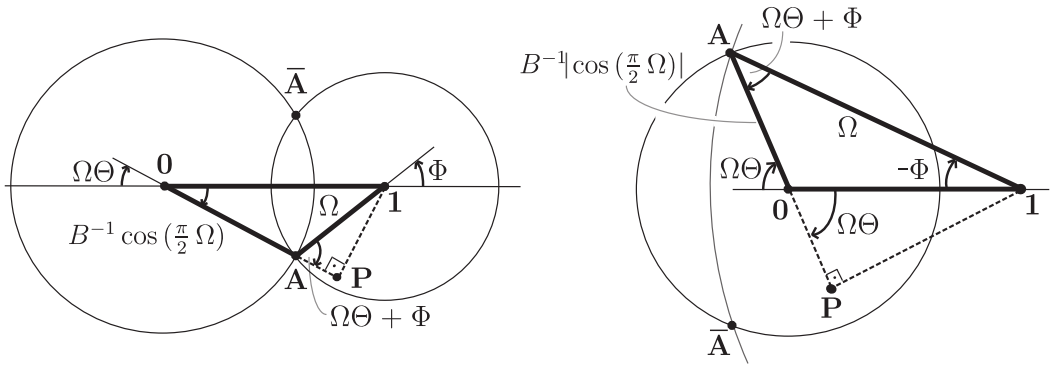

Figure 4.3: *Trigonometry of* (4.5)*. Left: the case* $0 < \Omega < 1$*. Right: the case* $1 < \Omega < 2$*. In either diagram we consider* $B \geq 1$ *in the domain* (4.8)*; see also fig. 4.2.*

The explicit expression (4.9) follows by explicit polar coordinates $(B,\, \Omega\Theta)$ from (4.5).

Real analytic dependence on $(\Omega,\, \Phi)$ holds for the expression (4.9) of B, Θ because positivity of B excludes $\cos(\frac{\pi}{2}\,\Omega) = 0$. The only possible exception is $\Omega = 1$ and $\Phi = 0$.

Similarly, real analytic dependence on $(\Omega,\, B)$ holds for the expression (4.7) of $\Phi,\, \Theta$. The only possible exception is the line $\Omega = 1,\, 0 < B < \pi/2$. Analyticity there, by continuation, will be shown in the next section. $\bowtie$

We cannot resist the temptation to include a geometric diversion here, which will become quite relevant in section 7.

Proposition 4.2. *Let* $\chi(\Omega,\, \Phi,\, \Theta,\, B) = 0$*, as in* (4.5)*, and assume*

$$0 < \Omega < 2, \quad \Omega \neq 1, \quad B \geq 1\,. \tag{4.10}$$

Then the following three estimates hold true:

$$\cos(\Omega\Theta + \Phi) > 0 \tag{4.11}$$

$$\sin(\Omega\Theta) \cdot \sin(\Omega\Theta + \Phi) > 0 \tag{4.12}$$

$$(1 - \Omega)\big(\cos(\Omega\Theta) - \Omega\cos(\Omega\Theta + \Phi)\big) > 0\,. \tag{4.13}$$

Proof. Joint sign reversal $\pm(\Phi,\, \Theta)$ or addition of multiples of 2π, separately, to $\Omega\Theta$ or Φ does not affect our claims. Therefore we may indeed assume the geometric situation of fig. 4.3 which holds for $B \geq 1$ and, respectively, for $0 < \Omega < 1$ and $1 < \Omega < 2$.

Consider $0 < \Omega < 1$ first. We show (4.11) first, i.e. the angle $\pi - (\Omega\,\Theta + \Phi)$ at $\mathbf{A}$ in the triangle $\mathbf{0A1}$ is obtuse. Comparing with Pythagoras we have to show, equivalently, that

$$\Omega^2 + B^{-2}\cos^2(\tfrac{\pi}{2}\Omega) < 1 \tag{4.14}$$

for all $B \geq 1$. For $0 < \Omega < 1$ this latter claim is equivalent to the trivial concavity assertion $\Omega < \sin(\frac{\pi}{2}\Omega)$. This proves (4.14), and (4.11). Claim (4.12) holds because the angles $\Omega\,\Theta$ and $\Omega\,\Theta + \Phi$ are between 0 and π.

Let the point $\mathbf{P}$ denote the orthogonal projection of $\mathbf{1}$ onto the straight line through $\mathbf{0A}$. See fig. 4.3, left. Then $\Omega\cos(\Omega\Theta + \Phi)$ is the length of $\mathbf{AP}$, because $\Omega\Theta + \Phi$ is the acute angle at $\mathbf{A}$ in the right-angled triangle $\mathbf{1AP}$; see (4.11). Clearly this length is shorter than the length $\cos(\Omega\Theta)$ of $\mathbf{0P}$. This proves (4.13).

Consider $1 < \Omega < 2$ next; see fig. 4.2, right. Again $\Omega\,\Theta$ and $\Omega\,\Theta + \Phi$ are between 0 and π, proving claim (4.12). Pythagoras and $1 < \Omega^2 + B^{-2}\cos^2\frac{\pi}{2}\Omega$ imply that the angle $0 < \Omega\,\Theta + \Phi < \pi/2$ at $\mathbf{A}$ in $\mathbf{1AP}$ is still acute. This proves (4.11).

To prove claim (4.13) we first show that the angle $\pi - \Omega\,\Theta$ at $\mathbf{0}$ in $\mathbf{A01}$ is obtuse. This follows by Pythagoras and $1 + B^{-2}\cos^2\frac{\pi}{2}\Omega < \Omega^2$, for $B \geq 1$, $1 < \Omega < 2$. In particular the length $\Omega\cos(\Omega\,\Theta + \Phi) > 0$ of $\mathbf{AP}$ exceeds the length $\cos\Omega\,\Theta$ of $\mathbf{0P}$, this time. Again this proves (4.13) and the proposition. ⋈

5 Expansions at Hopf resonance

In this section we study the scaled characteristic equation (4.5) in the limit $\Omega \to 1$. Since $\Omega = \omega\,\varepsilon = \omega/\omega_k$, by (4.1) and the 2-scale lift (4.4), the value $\Omega = 1$ indicates positions along the Hopf curves $\omega \mapsto (\vartheta(\omega),\, b(\omega))$ where the control-induced Hopf eigenvalue $\pm i\,\omega$ is in 1:1 resonance with the pinned primary Hopf eigenvalue $\pm i\,\omega_k$ of the supercritical Hopf bifurcation which we plan to stabilize. In lemma 5.2 we determine the curve in the $(\Theta,\, B)$-plane where this resonance $\Omega = 1$ occurs. In lemma 5.3 we determine the precise location of the 1:1 resonance in terms of ω, after hashing (4.4). We also determine an expansion, in terms of the small parameters $\Omega - 1$ and ε, of the nearest passages of the Hopf curves $\omega \mapsto (\vartheta(\omega),\, b(\omega))$ through the zero line $B = 1$. In section 9, this will provide the right and left boundaries $\gamma^{\iota}_{k,\,\pm}$ of the Pyragas regions $\mathcal{P}^{\iota}$, as announced in theorem 1.1. Our results are based on an expansion of the solutions

$$\Theta = \Theta\,(\Omega,\, B) \tag{5.1}$$

at $\Omega = 1$, in lemma 5.1.

Lemma 5.1. *With the continuation*

$$\begin{aligned} \Phi_{1,0} &:= 0\,, \\ \Theta_{1,0} &:= \arccos\,(2B/\pi) \end{aligned} \tag{5.2}$$

for $\Omega = 1,\, 0 < B < \frac{\pi}{2}$*, the expressions* (4.7) *for* $\Phi,\, \Theta$ *possess a unique real analytic extension to the domain* (4.8)*. Explicit first order expansions with respect to* $\Omega - 1$*,*

$$\begin{aligned} \pm\Phi &= \Phi_{1,0} + \Phi_{1,1} \cdot (\Omega - 1) + \dots\,, \\ \pm\Theta &= \Theta_{1,0} + \Theta_{1,1} \cdot (\Omega - 1) + \dots\,, \end{aligned} \tag{5.3}$$

are given by

$$\begin{aligned} \Phi_{1,1} &= -\sqrt{(\tfrac{\pi}{2}/B)^2 - 1}\,, \\ \Theta_{1,1} &= \sqrt{(\tfrac{\pi}{2}/B)^2 - 1} - \arccos\,(2B/\pi)\,. \end{aligned} \tag{5.4}$$

The expansions are uniform for B *in compact subsets of* $(0,\, \pi/2)$*.*

Proof. Analytic continuation for $\Omega \to 1$ of the expression (4.7) for Φ is obvious, by analyticity of the quotient $\cos\,(\frac{\pi}{2}\Omega)/(\Omega - 1) \to -\frac{\pi}{2}$. A similar analysis for the radicand of Θ provides the limit $(\frac{\pi}{2} - B)/(\frac{\pi}{2} + B)$ at $\Omega = 1$. This also completes the proof of the analyticity claims of lemma 4.1. The expansions (5.2) – (5.4) are straightforward, by symbolic or manual differentiation at $\Omega = 1$, if we use the elementary substitution

$$2\arctan\,\sqrt{\tfrac{1-\tau}{1+\tau}} = \arccos\,\tau \tag{5.5}$$

for $0 \le \tau := 2B/\pi \le 1$. This proves the lemma. ⋈

Lemma 5.2. *By analytic continuation through* $\Omega = 1$*, the solution set of the scaled characteristic equation* (4.5)*, i.e.*

$$\chi(1,\, \Phi,\, \Theta,\, B) = 0 \tag{5.6}$$

is given by

$$\Phi = 0, \qquad B = \tfrac{\pi}{2}\cos\,\Theta \tag{5.7}$$

for $|\Theta| < \pi/2$*.*

Proof. Analytic continuation through the geometrically singular configuration of fig. 4.3 at $\Omega = 1$ is established in lemma 4.1 and lemma 5.1. In particular (5.2) implies $\Phi = 0$ and proves claim (5.7). ⋈

We can now reinterpret our expansion of the solutions $(\Omega,\, \Phi,\, \Theta,\, B)$ of the scaled characteristic equation (4.5) near $\Omega = 1$ in terms of the original Hopf curves $(\vartheta(\omega),\, b(\omega))$ near the 1:1 resonance at $\omega = \omega_k$, alias $\Omega = 1$; see (3.3), (3.16). In terms of the scaled variables $(\Omega,\, \Phi,\, \Theta,\, B)$ of (4.3), (4.4) this means that we have to evaluate the solutions $(\Omega,\, \Phi,\, \Theta,\, B)$ along the hashing

$$\varepsilon^{-1}\Omega = \omega \equiv \Phi + (-1)^k \pi/2 \tag{5.8}$$

of (4.6), with the angle congruence $\Phi \pmod{2\pi}$ in S^1. This provides the *scaled Hopf curves*

$$\Omega \mapsto \big(\Theta(\Omega),\, B(\Omega)\big)\,. \tag{5.9}$$

Lemma 5.3. *Fix any nonzero integer $m \in \mathbb{Z}$ and consider*

$$\omega_{k+2m} - \tfrac{\pi}{2} \le \omega < \omega_{k+2m} + \tfrac{3}{2}\pi\,. \tag{5.10}$$

In scaled variables this corresponds to the hashing segment

$$\begin{aligned} -\tfrac{\pi}{2} \le \Phi = \omega - \omega_{k+2m} < \tfrac{3}{2}\pi \\ \Omega - 1 = (\Phi + 2\pi m)\,\varepsilon\,. \end{aligned} \tag{5.11}$$

Then the scaled Hopf curve solutions of the scaled characteristic equation (4.5) *satisfy*

$$\pm\Theta = \Theta(B) = \Theta_{1,\,0}(B) + 2\pi m\,\Theta_{1,\,1}(B)\,\varepsilon + \dots\,, \tag{5.12}$$

for $\varepsilon \searrow 0$, uniformly for B in compact subsets of $(0,\, \pi/2)$. See (5.2) – (5.4) *for the coefficients $\Theta_{1,\,0}$, $\Theta_{1,\,1}$.*

Proof. To show the hashing relation (5.11) between $\Omega - 1$ and Φ we first observe that

$$\Phi = 0 \quad \text{at} \quad \omega = \omega_k\,. \tag{5.13}$$

Indeed the hashing definition (4.6) with $\varepsilon = 1/\omega_k$ implies

$$\begin{aligned} \Phi &\equiv \Omega/\varepsilon + (-1)^{k+1}\pi/2 = (\Omega - 1)/\varepsilon + \omega_k + (-1)^{k+1}\pi/2 = \\ &= (\Omega - 1)/\varepsilon + \big(k + (1 + (-1)^{k+1})/2\big)\pi \\ &\equiv (\Omega - 1)/\varepsilon \pmod{2\pi}\,. \end{aligned} \tag{5.14}$$

Here we have used that the coefficient of π is even, for any parity of k. Inserting $\omega = \omega_k$, alias $\Omega = \omega/\omega_k = 1$, proves claim (5.13).

To show the hashing relation (5.11) for any nonzero integer m note that both Ω/ε and Φ coincide with ω, up to an additive constant. Since $\omega_{k+2m} = \omega_k + 2m\pi$, by definition (3.2) of $\omega_k = (k + 1/2)\pi$, this implies (5.11).

To show the shift (5.12) of the scaled Hopf curves, we invoke lemma 5.1 for Θ. Replacing $(\Omega - 1)$ in (5.3) by (5.11) we obtain

$$\pm\Theta = \Theta_{1,0}(B) + \Theta_{1,1}(B) \cdot (\Phi + 2\pi m)\,\varepsilon + \dots \tag{5.15}$$

with higher order terms of order $(\Omega - 1)^2$, alias ε^2. The expansion is uniform for B in compact subsets of $(0,\, \pi/2)$. But (5.3) also implies that Φ itself is of order at most $\Omega - 1$, alias ε, uniformly for such B. Indeed $\Phi_{1,0} = 0$. Therefore we may omit Φ in the expansion (5.15) and the lemma is proved. $\bowtie$

We conclude with a comment on the 1:1 Hopf resonance $\omega = \omega_k$, alias $\Omega = 1$, $\Phi = 0$. For $\omega \to \omega_k$, alias $\Omega - 1 \to 0$, $\Phi \to 0$, we naively combine the hashing (5.11) with expansion (5.3) at the excluded case $m = 0$:

$$\Omega - 1 = \Phi\,\varepsilon = \pm\Phi_{1,1}(B)\,\varepsilon\,(\Omega - 1) + \dots\,. \tag{5.16}$$

Cancelling $(\Omega - 1)$ on both sides leads to the illicit divergence $\Phi_{1,1}(B) = \pm\varepsilon^{-1} + \mathcal{O}(1)$ for $\varepsilon \searrow 0$. By further abuse of our derivation, (5.4) then implies

$$B = B_{1:1} := \pm\tfrac{\pi}{2}\varepsilon + \dots\,. \tag{5.17}$$

Direct inspection of the exact scaled characteristic equation (4.5) indeed verifies (5.17), and shows

$$\Theta = \Theta_{1:1} := 2\pi j \mp \tfrac{\pi}{2} + \dots \tag{5.18}$$

for any integer j. Alas, these resonances occur outside the region of interest for the Pyragas control near the zero line $B = 1$. In particular *the branch $m = 0$ of (5.12) is not a Hopf curve.* Rather $m = 0$, alias $\Omega = 1$, separates the Hopf curves for positive integer m from negative m, due to positivity of $\Theta_{1,1}(B)$ for $0 < B < \pi/2$. This observation also accounts for the resonance gap at $\Omega = 1$, alias $m = 0$, in the hashing region of fig. 4.2. Indeed $B \approx 0$ there, as derived in (5.17).

6 The Takens-Bogdanov Hopf curve

In this section we investigate the scaled Hopf curve

$$\Phi \mapsto \big(\Theta(\Phi),\, B(\Phi)\big) \tag{6.1}$$

which emanates from the Takens-Bogdanov point $(\vartheta_{\mathrm{TB}},\, b_{\mathrm{TB}})$ of (3.21), (3.22). In our scaling (4.3), (4.4) this corresponds to the limit

$$\begin{aligned} \Phi &\to \Phi_{\mathrm{TB}} := (-1)^{k+1}\pi/2 \\ \Omega\ &= \varepsilon(\Phi - \Phi_{\mathrm{TB}}) \to 0 \end{aligned} \tag{6.2}$$

which gives rise to the scaled limiting values

$$\Theta_{\mathrm{TB}} = (-1)^{k+1}, \qquad B_{\mathrm{TB}} = 1\,. \tag{6.3}$$

Similarly to lemma 5.1, where $\Omega = 1$, we now study the limit $\Omega = 0$. In lemma 6.1 we eliminate the trivial solution

$$\Omega = 0, \quad B = 1, \quad \Theta \in \mathbb{R} \tag{6.4}$$

which corresponds to the zero line (3.21) in scaled variables. In fact we replace B by the scaled variable β such that

$$B = 1 + \beta\,\Omega, \qquad \beta := (B-1)/\Omega\,, \tag{6.5}$$

and expand the solutions $(\Theta,\, \beta)$ of the scaled characteristic equation (4.5) in terms of $\Phi \in S^1$ and small $\Omega > 0$. In lemma 6.2 we collect the hashing consequences for the scaled Hopf curves, similarly to lemma 5.3.

Lemma 6.1. *Let $(\Theta,\, B)$ solve the scaled characteristic equation (4.5) and consider the scaled variable β of (6.5). Then $(\Theta,\, \beta)$ depend real analytically on $\Omega,\, \Phi \in S^1$, for sufficiently small $|\Omega|$. At $\Omega = 0$ we have the expansions*

$$\begin{aligned} \Theta &= \Theta_{0,\,0} + \Theta_{0,\,1}\Omega + \dots \\ \beta &= \beta_{0,\,0} + \beta_{0,\,1}\Omega + \dots \end{aligned} \tag{6.6}$$

with the explicit coefficients

$$\begin{aligned} \Theta_{0,\,0} &= \sin\,\Phi, \qquad & \Theta_{0,\,1} &= \tfrac{1}{2}\sin\,(2\Phi)\,, \\ \beta_{0,\,0} &= \cos\,\Phi, \qquad & \beta_{0,\,1} &= \tfrac{1}{4}\big(-\pi^2/2 + 1 + 3\cos\,(2\Phi)\big)\,. \end{aligned} \tag{6.7}$$

Proof. Inserting definition (6.5) of β into (4.5) we obtain equivalently

$$(1 + \beta\,\Omega)(1 - \Omega e^{i\,\Phi}) - 1 = \cos\,(\tfrac{\pi}{2}\Omega) e^{-i\,\Omega\Theta} - 1\,, \tag{6.8}$$

where both sides vanish identically for $\Omega = 0$. Dividing by Ω we obtain the analytic expression

$$\beta \cdot (1 - \Omega e^{i\,\Phi}) - e^{i\,\Phi} = \cos\,(\tfrac{\pi}{2}\Omega)(e^{-i\,\Omega\Theta} - 1)/\Omega + (\cos\,(\tfrac{\pi}{2}\Omega) - 1)/\Omega\,, \tag{6.9}$$

for small Ω. Indeed $\Omega = 0$ provides

$$\beta_0 + i\,\Theta_0 = e^{i\,\Phi}\,. \tag{6.10}$$

Differentiation at $\Omega = 0$ provides the remaining expressions of (6.7). ⋈

Lemma 6.2. *Consider the Hopf curve*

$$0 \le \omega \mapsto \big(\Theta(\omega),\, B(\omega)\big) \tag{6.11}$$

emanating from the Takens-Bogdanov point $\Theta_{\rm TB} = (-1)^{k+1}$, $B = 1$ *at* $\omega = 0$. *Then for* $\Omega = \varepsilon\omega \searrow 0$ *the following expansions hold true:*

$$\begin{aligned} (-1)^k\Theta &= -\cos\,\omega + \tfrac{1}{2}(-1)^k\varepsilon\omega\sin\,(2\omega) + \dots\,, \\ (-1)^k(B-1) &= \varepsilon\omega\sin\,\omega + \tfrac{1}{4}(-1)^k(\varepsilon\omega)^2\big(-\pi^2/2 + 1 - 3\cos\,(2\omega)\big) + \dots\,. \end{aligned} \tag{6.12}$$

In particular the tangent to the Hopf curve emanating at $\omega = 0$ *is given by the slope*

$$\frac{dB}{d\Theta} = 2\varepsilon + \dots\,. \tag{6.13}$$

Proof. We insert the hashing (4.4) into the expansion (6.5) – (6.7) of $(\Theta,\, B)$ with respect to $\Omega = \varepsilon\,\omega$. This proves the expansion (6.12). Letting $\omega \to 0$ in (6.12) proves the tangent (6.13), by cancellation of ω^2. This proves the lemma. ⋈

7 The zero line

In this section we investigate crossings of Hopf curves $\Omega \mapsto (\Theta(\Omega),\, B(\Omega))$ with the zero line $B = 1$. We use the explicit parametrization (4.7) of all solutions $(\Phi,\, \Theta)$ of the scaled characteristic equation (4.5) in terms of $(\Omega,\, B)$ in the domain (4.8); see also fig. 4.2. See fig. 7.1 for the graphs of Φ and Θ over Ω at $B = 1$. In lemma 7.2 we determine all crossings of the Hopf curves with the horizontal line $B = 1$, by hashing (4.6). In lemma 7.3 we study the directions in which the Hopf curves cross the horizontal line $B = 1$ when their frequency $\omega = \Omega\,\varepsilon^{-1} > 0$ increases. This will keep track of strict unstable dimensions E, later, upon crossing the Hopf lines along the zero line.

Specifically, the explicit solutions (4.7) of the characteristic equation (4.5) at the zero line $B = 1$ are given by $\pm(\Phi(\Omega),\, \Theta(\Omega))$ where

$$\begin{aligned} \Phi(\Omega) &:= 2\arctan\left[\,(1 - \Omega\sqrt{\frac{\cos^2(\frac{\pi}{2}\Omega)/(\Omega-1)^2 - 1}{(\Omega+1)^2 - \cos^2(\frac{\pi}{2}\Omega)}}\,\right], \\ \Theta(\Omega) &:= 2\,\Omega^{-1}\arctan\sqrt{\frac{\Omega^2 - (1-\cos\,\frac{\pi}{2}\Omega)^2}{(1+\cos\,\frac{\pi}{2}\Omega)^2 - \Omega^2}}\,. \end{aligned} \tag{7.1}$$

For $B = 1$ the domain (4.8) is $0 \le \Omega \le 2$. The Takens-Bogdanov limit $\Omega = 0$ is at $(-1)^{k+1}(\Phi(0),\, \Theta(0))$ with

$$\Phi(0) = \tfrac{\pi}{2}, \qquad \Theta(0) = 1\,. \tag{7.2}$$

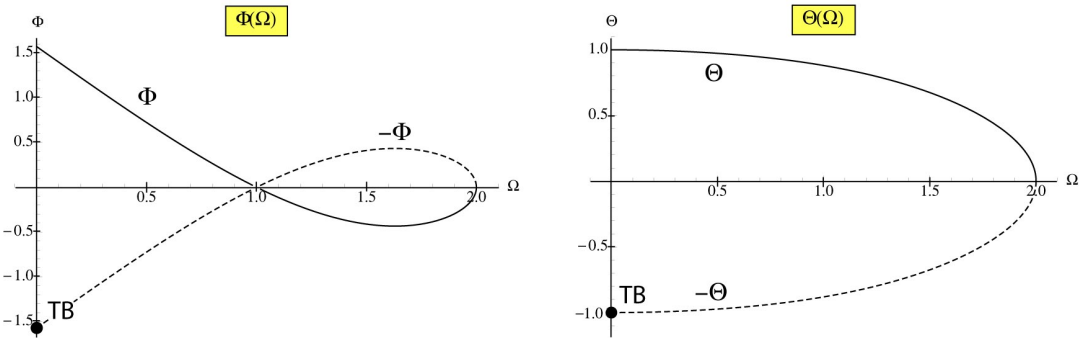

Figure 7.1: *The graphs of* $\Phi^{\pm}, \Theta^{\pm} = \pm(\Phi(\Omega), \Theta(\Omega))$ *of explicit solutions* (4.7) *for the scaled characteristic equation* (4.5) *evaluated along the zero line* $B = 1$. *Left:* $\Phi(\Omega)$*; right:* $\Theta(\Omega)$. *Solid and dashed graphs indicate positive and negative sign, respectively. Takens-Bogdanov points TB in the lower left corners, for even* k.

The limit at $\Omega = 2$ is given by

$$\Phi(2) = 0, \qquad \Theta(2) = 0\,. \tag{7.3}$$

We have taken $-\frac{\pi}{2} \le \Phi < \frac{3}{2}\pi \bmod 2\pi$ and we have omitted branches $\pm\Theta + 2\pi j/\Omega$ for nonzero integer j, which are outside our region of interest.

We prepare for the lemmas with a proposition on elementary properties of the trigonometric functions $\Phi(\Omega)$, $\Theta(\Omega)$. While the expansions are symbolic and exact, we were unable to prove our convexity and monotonicity claims on Φ and Θ. Readers with a lot of spare time are encouraged to try. Instead we "verified" these claims by checking the signs of $\Phi''(\Omega)$ and $\Theta'(\Omega)$ against high precision numerical evaluations of the symbolic derivatives at 10^6 equidistant points in each of the intervals $0 < \Omega < 1$ and $1 < \Omega < 2$.

Proposition 7.1. *Let* $0 \le \Omega \le 2$.

(i) We obtain the following expansions for $\Phi(\Omega)$, $\Theta(\Omega)$ *in* (7.1) *at* $\Omega = 0$, 1, 2, *respectively. Omitted higher order terms are of order one higher than the last written term, except where indicated otherwise.*

$$\begin{aligned} \Phi(\Omega) &= \tfrac{\pi}{2} - \tfrac{1}{2}\big((\tfrac{\pi}{2})^2 + 1\big)\Omega + \tfrac{1}{48}\big(-(\tfrac{\pi}{2})^6 + 5(\tfrac{\pi}{2})^4 - 3(\tfrac{\pi}{2})^2 - 1\big)\Omega^3 + \dots \\ \Theta(\Omega) &= 1 - \tfrac{1}{24}\big(3(\tfrac{\pi}{2})^4 - 6(\tfrac{\pi}{2})^2 - 1\big)\Omega^2 + \mathcal{O}(\Omega^4) \end{aligned} \tag{7.4}$$

$$\begin{aligned} \Phi(\Omega) &= -\sqrt{(\tfrac{\pi}{2})^2 - 1}\,(\Omega - 1) + \sqrt{(\tfrac{\pi}{2})^2 - 1}\,(\Omega - 1)^2 + \\ &\quad + \frac{3(\tfrac{\pi}{2})^4 - 7(\tfrac{\pi}{2})^2 + 8}{24\sqrt{(\tfrac{\pi}{2})^2 - 1}}\,(\Omega - 1)^3 + \dots \\ \Theta(\Omega) &= \arccos\tfrac{2}{\pi} + \big(\tfrac{1}{2}\sqrt{(\tfrac{\pi}{2})^2 - 1} - \arccos\tfrac{2}{\pi}\big)(\Omega - 1) + \dots \end{aligned} \tag{7.5}$$

$$
\begin{aligned}
\Phi(\Omega) &= -(2-\Omega)^{1/2} + \tfrac{1}{24}\big(6(\tfrac{\pi}{2})^2 - 1\big)(2-\Omega)^{3/2} + \\
&\quad + \tfrac{1}{640}\big(20(\tfrac{\pi}{2})^4 + 100(\tfrac{\pi}{2})^2 - 3\big)(2-\Omega)^{5/2} + \dots \\
\Theta(\Omega) &= (2-\Omega)^{1/2} - \tfrac{1}{24}\big(6(\tfrac{\pi}{2})^2 - 13\big)(2-\Omega)^{3/2} - \\
&\quad - \tfrac{1}{1920}\big(60(\tfrac{\pi}{2})^4 + 60(\tfrac{\pi}{2})^2 - 529\big)(2-\Omega)^{5/2} + \dots
\end{aligned}
\tag{7.6}
$$

(ii) By numerical evidence for $0 < \Omega < 2$,

$$
\Phi''(\Omega) > 0 > \Theta'(\Omega)\,. \tag{7.7}
$$

(iii) We have the estimates

$$
\begin{aligned}
0 \le \Theta(\Omega) &\le 1 \\
-0.4336\ldots \le \Phi(\Omega) &\le \pi/2\,.
\end{aligned}
\tag{7.8}
$$

Proof. The symbolic expansions of (7.4), (7.5) are straightforward, e.g. by any symbolic package. The factor $\sqrt{2-\Omega}$ in the expansions (7.6) is generated by the numerators inside the square roots of (7.1). Here we conveniently multiply that numerator in $\Phi(\Omega)$ by $(\Omega-1)^2$. This proves (i).

We already pointed out how we "verified" (iii) numerically, for lack of improper stamina.

The estimate (7.8) for $\Theta(\Omega)$ follows from the limits $\Theta(0) = 1$, $\Theta(2) = 0$ in (i) and monotonicity (ii). Similarly, strict convexity of Φ and the limits $\Phi(0) = \pi/2$, $\Phi(2) = 0$, $\Phi'(0) = -(\pi^2+4)/8$, $\Phi'(2) = +\infty$ prove the upper estimate $\Phi(\Omega) \le \pi/2$. The lower estimate is obtained by numerical approximation of the unique minimum at $\Phi'(\Omega) = 0$. In fact the minimizer Ω is given by solving the transcendental equation

$$
\Omega^2 - \sin^2(\Omega\pi/2) + \sin(\Omega\pi)\cdot\Omega\pi/2 = 0 \tag{7.9}
$$

for $1 < \Omega < 2$. ⋈

To determine all crossing points Θ of Hopf curves $\Omega \mapsto (\Theta(\Omega),\, B(\Omega))$ with the zero line $B = 1$ we recall the hashing (4.6) in the form

$$
\varepsilon^{-1}\,\Omega = \omega = \omega_{k+2m} + \Phi\,, \tag{7.10}
$$

where m is integer and $-\pi/2 \le \Phi < 3\pi/2$. Here we have used $\Phi = 0$ at $\omega = \omega_k = 1/\varepsilon$, $\Omega = 1$; see (5.13). We also used $\omega_{k+2m} = \omega_k + 2m\pi$ for $\omega_k := (k+\frac{1}{2})\pi$; see (3.2). The constraint $\omega \ge 0$ then translates to

$$
\begin{aligned}
m \ge \underline{m} &:= -k/2, && \text{for even} \quad k\,, \\
m \ge \underline{m} &:= -(k+1)/2, && \text{for odd} \quad k
\end{aligned}
\tag{7.11}
$$

in (7.10). For odd k and $m = \underline{m}$ we have the additional constraint $\Phi \geq \pi/2$. The constraint $\Omega < 2$ alias $\omega < 2\omega_k$, on the other hand, translates to

$$\begin{aligned} &m \leq \overline{m} := k/2, && \text{for even} \quad k\,, \\ &m \leq \overline{m} := (k-1)/2, && \text{for odd} \quad k\,. \end{aligned} \tag{7.12}$$

For even k and $m = \overline{m}$ we have the additional constraint $\Phi < \pi/2$. Note $\underline{m} = [-k/2]$, $\overline{m} = [k/2]$ for all k, where $[\,\cdot\,]$ is the floor function.

Lemma 7.2. *Any intersection of the Hopf curves $(\Theta(\Omega), B(\Omega))$ with the zero line $B = 1$ in the region $|\Theta| < \pi - 1$ occurs for some $0 \leq \Omega < 2$.*

More precisely, a complete list of intersection points is given as follows. For $0 < |m| \leq \overline{m}$, each interval $\omega_{k+2m} - \pi/2 \leq \omega < \omega_{k+2m} + 3\pi/2$ contains exactly two intersection points

$$\varepsilon^{-1}\,\Omega^{\pm}_{k+2m} = \omega^{\pm}_{k+2m} = \omega = \omega_{k+2m} + \Phi^{\pm}_{k+2m}\,. \tag{7.13}$$

The only exception is the additional case $m = -\underline{m} = -(k+1)/2$ for odd k, where $\Omega^{+}_{-1} = 0$ is the Takens-Bogdanov point at $\Phi^{+}_{-1} = +\pi/2$, and Ω^{-}_{k+2m} is absent. For even k and $m = -\overline{m}$ we obtain the Takens-Bogdanov point $\Omega^{-}_{0} = 0$ at $\Phi^{-}_{0} = -\pi/2$.

In general $|\Phi^{\pm}_{k+2m}| \leq \pi/2$ because

$$\Phi^{\pm}_{k+2m} = \pm\Phi(\Omega^{\pm}_{k+2m})\,. \tag{7.14}$$

The crossings occur at

$$\Theta^{\pm}_{k+2m} = \pm\Theta(\Omega^{\pm}_{k+2m})\,, \tag{7.15}$$

and hence for $|\Theta| \leq 1$. For negative m, the ordering of the ω-values is given by

$$0 \leq \ldots < \omega^{-}_{k+2m} < \omega_{k+2m} < \omega^{+}_{k+2m} < \omega_{k+2m+1} < \omega^{-}_{k+2m+2} < \ldots < \omega_k\,. \tag{7.16}$$

For positive m, the $\pm$-order is reversed:

$$\omega_k < \ldots < \omega^{+}_{k+2m} < \omega_{k+2m} < \omega^{-}_{k+2m} < \omega_{k+2m+1} < \omega^{+}_{k+2m+2} < \ldots < 2\omega_k\,. \tag{7.17}$$

Of course $0 \leq \Omega^{\pm}_{k+2m} = \varepsilon\,\omega^{\pm}_{k+2m} < 2$ are ordered analogously. The absolute values $|\Theta^{\pm}_{k+2m}|$ are ordered strictly oppositely to $\Omega^{\pm}_{k+2m}$, i.e. they are ordered as $-\Omega^{\pm}_{k+2m}$ are. More precisely

$$\begin{aligned} &-1 \leq \ldots < \Theta^{-}_{k-2m} < -\Theta^{+}_{k-2m} < \Theta^{-}_{k-2(m-1)} < \ldots < -\arccos\tfrac{2}{\pi}\,, \\ &-\arccos\tfrac{2}{\pi} < \ldots < \Theta^{-}_{k+2m} < -\Theta^{+}_{k+2m} < \Theta^{-}_{k+2(m+1)} < \ldots < 0\,, \end{aligned} \tag{7.18}$$

for positive m as in (7.12). For $0 < \Theta \leq +1$ these orders are reversed.

With the abbreviation $q{:=}\ \arccos 2/\pi$ *of* (1.14) *and for* $m = \pm 1$ *we have the expansions*

$$\begin{aligned} \Omega^{\iota}_{k\pm 2} &= 1 \pm 2\pi\,\varepsilon + \dots \\ \iota\,\Phi^{\iota}_{k\pm 2} &= \iota\,\Phi(\Omega^{\iota}_{k\pm 2}) = \mp 2\pi\sqrt{(\tfrac{\pi}{2})^2 - 1}\,\varepsilon + \dots \\ \iota\,\Theta^{\iota}_{k\pm 2} &= \iota\,\Theta(\Omega^{\iota}_{k\pm 2}) = q \pm \pi\big(\sqrt{(\tfrac{\pi}{2})^2 - 1} - 2q\big)\,\varepsilon + \dots \end{aligned} \tag{7.19}$$

Here $\iota = \pm$ *and* $\varepsilon^{-1} = \omega_k = (k + \frac{1}{2})\pi \to +\infty$, *i.e.* $\varepsilon \to 0$.

Proof. We address the general case $0 < |m| \le \overline{m}$ and leave the interesting but special Takens-Bogdanov case to the eager reader. The bound $|\Theta^{\pm}(\Omega)| \le 1$ fixes the primary branch $j = 0$ in the region $|\Theta| < \pi - 1$, $0 \le \Omega \le 2$ of our interest; see (7.1).

To obtain the intersections Ω^{+}_{k+2m} we first solve the hashing relation (7.13) for Ω, i.e.

$$\Phi(\Omega) \equiv \varepsilon^{-1}\Omega - \omega_{k+2m} \equiv \varepsilon^{-1}(\Omega - 1) \pmod{2\pi}\,. \tag{7.20}$$

Here we have used $\omega_{k+2m} = \omega_k + 2m\pi$, again, and $\varepsilon\,\omega_k = 1$. Because $\Phi(2) = 0$ and $\varepsilon^{-1} = \omega_k \equiv \pm\pi/2 \,(\mathrm{mod}\, 2\pi)$, crossing does not occur at $\Omega = 2$.

By proposition 7.1, $\Phi(\Omega)$ is convex with bounded $\Phi'(0) < 0$ and $\Phi'(2) = +\infty$. This proves uniqueness of the solution $\Omega^{+}_{k+2m}{:=}\ \Omega$ of (7.20). Moreover $\Phi(\Omega) > 0$ for $0 \le \Omega < 1$ implies $\Omega^{+}_{k+2m} > \Omega_{k+2m}{:=}\ \varepsilon\,\omega_{k+2m}$, for $m < 0$ alias $\Omega_{k+2m} < 1$. Similarly $\Phi(\Omega) < 0$ for $1 < \Omega < 2$, after the unique sign change of Φ at $\Omega = 1$, implies $\Omega^{+}_{k+2m} < \Omega_{k+2m}$ for $m > 0$. The remaining intersections $\Omega = \Omega^{-}_{k+2m}$ with the negative branch $-\Phi(\Omega)$ are obtained analogously and prove the inequalities (7.16), (7.17) except for one additional detail. We use $|\Phi(\Omega)| \le \pi/2$, for $0 \le \Omega \le 2$, to show the remaining inequalities

$$\begin{aligned} \omega^{+}_{k+2m} &= \omega_{k+2m} + \Phi^{+}_{k+2m} \le \omega_{k+2m} + \pi/2 < \omega_{k+2m+1} < \\ &< \omega_{k+2(m+1)} - \pi/2 \le \omega_{k+2(m+1)} + \Phi^{-}_{k+2(m+1)} = \omega^{-}_{k+2(m+1)}\,, \end{aligned} \tag{7.21}$$

for $m < 0$, and similarly for $m > 0$. The bounds $|\Phi(\Omega)| \le \pi/2$ and $|\Theta(\Omega)| \le 1$ also follow from proposition 7.1, along with strict monotonicity of $\Theta^{\pm}(\Omega) = \pm\Theta(\Omega)$.

To prove the expansions (7.19) we fix $m = \pm 1$. From the hashing (7.20) we obtain

$$\varepsilon = \varepsilon(\Omega) := (\Omega - 1)/(\iota\,\Phi(\Omega) + 2m\pi)\,, \tag{7.22}$$

where $\iota = \pm$. The right hand side defines a series expansion

$$\varepsilon^{\iota}_{\pm}(\Omega) = \big(\iota\,\Phi(1) + 2m\pi\big)^{-1}(\Omega - 1) + \dots \tag{7.23}$$

for $\varepsilon^{\iota}_{\pm}(\Omega)$, with $\Phi(1) = 0$. Inverting this expansion as $\Omega^{\iota}_{k+2m} = \Omega^{\iota}_{m}(\varepsilon) = 1 + 2m\pi\varepsilon + \dots$ we obtain the expansions for $\Omega^{\iota}_{k\pm 2}$ in (7.19). Substituting the resulting series in the expansions (7.5) for $\Phi(\Omega)$, $\Theta(\Omega)$ at $\Omega = 1$ proves the remaining expansions of (7.19), and the lemma. $\bowtie$

Lemma 7.3. *Let $\varepsilon > 0$ be small enough and consider the region $|\Theta| < \pi - 1$.*

Then all crossings of Hopf curves $\omega \mapsto (\Theta(\omega),\, B(\omega))$ with the zero line $B = 1$ are transverse with nonvanishing slope. The direction of the crossing is given by

$$\operatorname{sign} B'(\omega) = \iota \operatorname{sign} m\,, \qquad \operatorname{sign} \Theta'(\omega) = -\operatorname{sign} m\,, \tag{7.24}$$

at any crossing $\varepsilon\omega = \Omega^{\iota}_{k+2m}$, $\Theta = \Theta^{\iota}_{k+2m}$, $\iota = \pm$, of the Hopf curve; see lemma 7.2.

Proof. Let $'$ denote derivatives with respect to ω at any Hopf crossing. Let subscripts denote partial derivatives of the characteristic function χ of (4.5) at any crossing. By implicit differentiation of

$$\chi\big(\Omega(\omega),\, \Phi(\omega),\, \Theta(\omega),\, B(\omega)\big) = 0 \tag{7.25}$$

at $\chi = 0$, $B = 1$ we obtain

$$\varepsilon\, \chi_\Omega + \chi_\Phi + \chi_\Theta \cdot \Theta' + \chi_B \cdot B' = 0\,. \tag{7.26}$$

Here we have used $\Omega' = \varepsilon$ and $\Phi' = 1$. Note $|\chi_\Omega| \le C$ is uniformly bounded. To solve (7.26) for Θ', B' let us consider the limiting case $\varepsilon = 0$ first. A subsequent discussion of the case of small $\varepsilon > 0$ will complete the proof.

For solutions of $\chi = 0$ on the zero line $B = 1$ we obtain the partial derivatives

$$\begin{aligned} \chi_\Phi &= -i\,\Omega\, e^{i\,\Phi}\,, \\ \chi_\Theta &= i\,\Omega\, \cos\left(\tfrac{\pi}{2}\Omega\right) e^{-i\,\Omega\Theta}\,, \\ \chi_B &= \cos\left(\tfrac{\pi}{2}\Omega\right) e^{-i\Omega\Theta}\,. \end{aligned} \tag{7.27}$$

Inserting (7.27) into (7.26) with $\varepsilon := 0$ we obtain

$$\cos\left(\tfrac{\pi}{2}\Omega\right)(B' + i\,\Omega\Theta') = i\,\Omega\, e^{i(\Omega\Theta+\Phi)}\,. \tag{7.28}$$

For $0 < \Omega < 2$ and $\Omega \neq 1$ this implies

$$\begin{aligned} B' &= \frac{-\Omega}{\cos\left(\frac{\pi}{2}\Omega\right)}\, \sin\left(\Omega\Theta + \Phi\right) \\ \Theta' &= \frac{1}{\cos\left(\frac{\pi}{2}\Omega\right)}\, \cos\left(\Omega\Theta + \Phi\right) \end{aligned} \tag{7.29}$$

both exist with crossing slope

$$\frac{dB}{d\Theta} = -\Omega\, \tan\left(\Omega\Theta + \Phi\right). \tag{7.30}$$

Inserting $(\Phi,\, \Theta) = (\Phi^\iota(\Omega),\, \Theta^\iota(\Omega)) = \iota\,(\Phi(\Omega),\, \Theta(\Omega))$ for $\iota = \pm$, and observing the appropriate signs, (7.29) implies

$$\operatorname{sign} B' = -\iota \operatorname{sign}(1 - \Omega) = \iota \operatorname{sign} m\,, \qquad \operatorname{sign} \Theta' = -\operatorname{sign} m\,. \tag{7.31}$$

Here we have used sign $\cos\frac{\pi}{2}\Omega = \operatorname{sign}(1-\Omega)$, $\operatorname{sign}\Theta^\iota = \iota$, and the geometric properties (4.11), (4.12) of proposition 4.2 with $\operatorname{sign}\sin\Omega\,\Theta^\iota = \iota$.

For small $\varepsilon > 0$, our argument breaks down in $C\,\varepsilon$-neighborhoods of $\Omega = 0$, only. Indeed $|\chi_\Phi| = \Omega$ dominates the term $\varepsilon\,\chi_\Omega$ elsewhere. The neighborhood of $\Omega = 0$, however, has already been studied in section 6. In particular the expansions of lemma 6.2 confirm (7.24) in this region.

Near $\Omega = 1$, $\Omega\Theta + \Phi = \pm\arccos 2/\pi$, the crossing occurs at large speed in the parameter ω, but the approximations (7.29), (7.30) of crossing direction and slope remain valid. For $\Omega \nearrow 2$, finally, the crossing becomes nearly tangent but the approximation (7.29) remains valid for $\varepsilon \searrow 0$, because $\varepsilon\,|\chi_\Omega| << |\chi_\Phi|$. This proves the lemma. ⋈

8 The line of neutral Hopf tangencies

As a final preparation for our proof of theorems 1.1 and 1.2 we study the intersections of Hopf curves with the half line $\Theta = 0$, $B \geq 1$. This reduces the scaled characteristic equation (4.5) to

$$0 = \chi(\Omega,\,\Phi,\,\Theta = 0,\,B) = 1 - \Omega\,e^{i\,\Phi} - B^{-1}\cos\left(\tfrac{\pi}{2}\Omega\right). \tag{8.1}$$

In lemma 8.1 we identify all such intersections $(\Omega,\,\Phi,\,B)$ with $B \geq 1$. In lemma 8.2 we show that all intersections are transverse. In fact each intersection is used by two different Hopf curves at $\Omega = 1 \pm 2\,\widetilde{\Omega}/\pi$ which cross with the same near-horizontal tangent, but in opposite directions. See also figs. 1.2, 4.1, 10.1. To emphasize this symmetry we also express our results in terms of

$$\widetilde{\Omega} := \tfrac{\pi}{2}(\Omega - 1)\,, \qquad \Omega = 1 + 2\,\widetilde{\Omega}/\pi\,. \tag{8.2}$$

Lemma 8.1. *All solutions of the characteristic equation* (4.5) *with* $\Theta = 0$ *and* $B \geq 1$ *satisfy* $\Phi \equiv 0 \,(\mathrm{mod}\, 2\pi)$ *and*

$$0 < \Omega < 2\,, \qquad \Omega \neq 1\,. \tag{8.3}$$

In particular the solutions are given by the equivalent expressions

$$\begin{aligned} \omega &= \omega_{k+2m} = \omega_k + 2m\pi \\ \Omega &= \Omega_{k+2m} := \omega_{k+2m}/\omega_k = 1 + 2m\pi/\omega_k \\ \widetilde{\Omega} &= \widetilde{\Omega}_{2m} := \tfrac{m}{k+1/2}\,\pi \end{aligned} \tag{8.4}$$

with integers m *such that*

$$0 < |m| \leq \overline{m} = [k/2]\,. \tag{8.5}$$

The crossings occur at the levels

$$B = B_{k+2m} := \frac{\cos\left(\frac{\pi}{2}\Omega_{k+2m}\right)}{1-\Omega_{k+2m}} = \frac{\pi}{2}\,\frac{\sin\widetilde{\Omega}_{2m}}{\widetilde{\Omega}_{2m}} \in (1,\,\tfrac{\pi}{2})\,. \tag{8.6}$$

In particular the levels $B_{k-2m} = B_{k+2m}$ *coincide because* $\widetilde{\Omega}_{-2m} = -\widetilde{\Omega}_{2m}$.

Proof. From the domain (4.8) we conclude

$$0 \le \Omega \le 2 \tag{8.7}$$

for $B \ge 1$. To prove claim (8.3) we successively exclude the cases $\Omega \in \{0,\,1,\,2\}$.

We recall that $\Omega = 0$ marks the Takens-Bogdanov point $\Theta = \Theta_{\rm TB} = (-1)^{k+1} \neq 0$, $B = B_{\rm TB} = 1$; see (3.22), (4.3). Therefore we only consider $\Omega > 0$ and conclude $\Phi \equiv 0$ or $\Phi \equiv \pi \mod 2\pi$ from (8.1).

Suppose $\Phi \equiv \pi$. Then (8.1) implies $B = \cos\left(\frac{\pi}{2}\Omega\right)/(1+\Omega) < 1$, which is outside our domain $B \ge 1$ of interest (but could easily be analyzed, as well). This proves $\Phi \equiv 0$.

For $\Phi \equiv 0 \mod 2\pi$, which holds at $\omega = \omega_k$ by (5.13), hashing (4.4) implies

$$\omega = \omega_{k+2m} = \omega_k + 2m\pi \tag{8.8}$$

for some integer m; see (8.4). This cannot hold at $\omega = 2\omega_k = \omega_k + (k+1/2)\pi$, alias $\Omega = 2$. Hence we only have solutions $\Omega < 2$.

At $1 = \Omega = \omega/\omega_k$, alias $m = 0$, we encounter the 1:1 resonance at $\Theta_{1:1} = 2\pi j \mp \pi/2 \neq 0$, $B_{1:1} = \pm\frac{\pi}{2}\,\varepsilon + \ldots$; see (5.17). Again this is excluded at $\Theta = 0$. This shows that Hopf intersections with the half line $\Theta = 0$, $B \ge 1$ can only occur for $\Phi \equiv 0\,(\mathrm{mod}\,2\pi)$ and $0 < \Omega < 2$, $\Omega \neq 1$. This proves claim (8.3).

Substituting $\omega = \Omega/\varepsilon = \Omega\,\omega_k$ and (8.2) into (8.8) proves (8.4), (8.5). Solving (8.1) for B proves (8.6), and the lemma. ⋈

Lemma 8.2. *In the setting of lemma 8.1 consider the intersections* $\omega = \omega_{k+2m}$, $0 < |m| \le \overline{m} = [k/2]$ *of the Hopf curves* $\omega \mapsto (\Theta(\omega),\,B(\omega))$ *with the half line* $\Theta = 0$, $B \ge 1$. *Let* $'$ *denote derivatives with respect to the frequency parameter* ω. *Then all intersections are transverse crossings with the exact derivatives*

$$\begin{aligned} \Theta' &= -\tfrac{\pi}{2}/\widetilde{\Omega}\,, \\ B' &= -\varepsilon\,(\tfrac{\pi}{2})^2(\sin\widetilde{\Omega} - \widetilde{\Omega}\cos\widetilde{\Omega})/\widetilde{\Omega}^2\,. \end{aligned} \tag{8.9}$$

Here $\widetilde{\Omega} = \widetilde{\Omega}_{2m}$ *as given in* (8.4), (8.5), *and hence* $0 < |\widetilde{\Omega}| < \pi/2$. *In particular crossings occur* in opposite directions *by opposite signs of* $\widetilde{\Omega} = (\Omega-1)\pi/2$ *at* $\widetilde{\Omega}_{-m} = -\widetilde{\Omega}_m$; *see* (8.4). *The exact crossing slopes coincide at* $\widetilde{\Omega} = \pm\widetilde{\Omega}_m$:

$$\frac{dB}{d\Theta} = \varepsilon\,\tfrac{\pi}{2}(\sin\widetilde{\Omega} - \widetilde{\Omega}\cos\widetilde{\Omega})/\widetilde{\Omega}\,. \tag{8.10}$$

Note how the near-horizontal crossing slopes are uniformly small of order ε.

Proof. Analogously to (7.27) in the proof of lemma 7.3, we calculate

$$
\begin{aligned}
\chi_\Omega &= -1 + \tfrac{\pi}{2} B^{-1} \cos \widetilde{\Omega} \\
\chi_\Phi &= -i\,\Omega \\
\chi_\Theta &= -i\,\Omega \cdot \widetilde{\Omega}/\tfrac{\pi}{2} \\
\chi_B &= -B^{-1} \cdot \widetilde{\Omega}/\tfrac{\pi}{2}
\end{aligned}
\tag{8.11}
$$

for the characteristic function χ at $\Theta = 0$, $\Phi = 0$, $B = \cos(\frac{\pi}{2}\Omega)/(1-\Omega)$. By implicit differentiation as in (7.25), (7.26) we obtain $\Theta' = -\chi_\Phi/\chi_\Theta = -\frac{\pi}{2}/\widetilde{\Omega}$ and $B' = -\varepsilon\chi_\Omega/\chi_B$. Substitution of $\widetilde{\Omega}$ for Ω and $B = \cos(\frac{\pi}{2}\Omega)/(1-\Omega) = \frac{\pi}{2}\widetilde{\Omega}^{-1}\sin\widetilde{\Omega}$, as in (8.6), proves (8.9), (8.10), and the lemma. ⋈

9 Proof of theorems 1.1 and 1.2

Using the results of sections 2 – 8, we are now ready to prove our main results, theorems 1.1 and 1.2. We first identify the Pyragas region

$$
\mathcal{P}_k = \mathcal{P}_k^+ \cup \mathcal{P}_k^- : \qquad E(\Theta,\, B) = 0 \tag{9.1}
$$

of parameters $(\vartheta,\, b)$ in the scaled variables $(\Theta,\, B)$ of (4.3). We recall from (3.4) that E counts the total algebraic multiplicity of eigenvalues μ with $\operatorname{Re}\mu > 0$ at the bifurcation point $\lambda = \lambda_k$ of supercritical Hopf bifurcation, as identified in section 2.

In lemma 9.2 we show how each region $\mathcal{P}_k^\iota$ is bounded by four curves

$$
\mathcal{P}_k^\iota : \qquad B = 1\,; \quad \Gamma_k^0\,; \quad \Gamma_{k,\,\pm}^\iota\,; \tag{9.2}
$$

for $\iota = \pm$ and large enough k. Here $B = 1$ is the zero line of an eigenvalue $\mu = 0$ studied in lemma 3.4 and section 7. The Hopf curves $\Gamma_{k,\,\pm}^\iota$ are the Hopf curves which cross the zero line $B = 1$ transversely at

$$
\Theta = \Theta_{k\pm2}^\iota = \iota\left(q \pm \pi\big(\sqrt{(\tfrac{\pi}{2})^2 - 1} - 2q\big)\,\varepsilon + \ldots\right), \tag{9.3}
$$

according to lemmas 7.2 and 7.2. Here $q = \arccos 2/\pi = 0.88\ldots < 1$. The Takens-Bogdanov Hopf curve Γ_k^0, restricted to parameters $0 < \omega < \pi$, was studied in section 6; see lemma 6.2 in particular.

In lemma 9.1 we determine

$$
E(\Theta = \iota q,\, B = 1) = 0 \tag{9.4}
$$

on the zero line $B = 1$ bounding the region $\mathcal{P}_{k,\,\pm}^\iota$. By expansion (6.12) of the Takens-Bogdanov Hopf curve Γ_k^0 we have

$$
\operatorname{sign}(B-1) = (-1)^k \tag{9.5}
$$

in the Pyragas regions $\mathcal{P}_k^\iota$. At $\Theta = \iota q$ the crossing direction (3.23) of the critical eigenvalue $\mu = 0$ is given by

$$\begin{aligned} \operatorname{sign} \partial_B \mu(\Theta,\, B=1) = (-1)^k \operatorname{sign} \partial_b \mu(\vartheta,\, b_{\mathrm{TB}}) = \operatorname{sign}(\vartheta_{\mathrm{TB}} - \vartheta) = \\ = \operatorname{sign}(\Theta_{\mathrm{TB}} - \Theta) = \operatorname{sign}\big((-1)^{k+1} - \iota q\big) = (-1)^{k+1}\,. \end{aligned} \tag{9.6}$$

Here we have used scaling (4.3) and (6.3). The crossing direction (9.6) combines with (9.4) to prove $E(\Theta,\, B) = 0$ in the Pyragas region $\mathcal{P}_k = \mathcal{P}_k^+ \cup \mathcal{P}_k^-$ of (9.1).

To complete the proofs of theorems 1.1, 1.2 we rewrite the boundary curves (9.2) of $\mathcal{P}_k$, and their expansions, in terms of the original control variables $(\vartheta,\, b)$; see lemma 9.3.

Lemma 9.1. *In the above notation*

$$E(\Theta = 0,\, B = 1) = \begin{cases} k, & \text{for even} \quad k\,, \\ k-1, & \text{for odd} \quad k\,. \end{cases} \tag{9.7}$$

For $\iota = \pm$ and small enough $0 < \varepsilon = 1/\omega_k$ this implies $E(\Theta = \iota q,\, B = 1) = 0$, as claimed in (9.4).

Proof. We apply the jump property (3.18) in the $(\Theta,\, B)$-plane with $B > 0$. The orientations of ϑ and Θ coincide. The substitution $b = (-1)^k\, 2B\,\varepsilon$ switches the orientation of b, but also the right and the left sides of non-vertical Hopf curves, for odd k. Therefore (3.18) implies the jump property

$$[\, E(\Theta,\, B)\,]_{\mathrm{left}}^{\mathrm{right}} = -2 \tag{9.8}$$

for all $B > 0$.

To prove claim (9.7) we apply the jump property (9.8) along the vertical half line $\Theta = 0$, $B \geq 1$. At $B = +\infty$, alias $b = \infty$, instability property (3.6) implies $E(\Theta = 0,\, B = +\infty) = E(\lambda_k) = k$. Decreasing B from $+\infty$ to 1 along the half line, lemma 8.1 reveals a finite sequence of $[\,k/2\,]$ Hopf curves, which intersect in pairs at decreasing levels $B = B_{k-2m} = B_{k+2m} \in (1,\, \pi/2)$ for $m = 1,\, \ldots,\, [\,k/2\,]$. By lemma 8.2 each pair crosses the half line $\Theta = 0$ transversely, and even with the same tangent, but in opposite directions. Therefore the contribution of each pair to the jumps (9.8) cancels. In consequence $E(\Theta = 0,\, B) = k$ for small enough $0 < B - 1 << 1$ below the last crossing at $m = [\,k/2\,]$. Invoking (9.6) at $\Theta = 0$, instead of $\Theta = \iota q$, proves claim (9.7).

To prove claim (9.4) we continue our itinerary from $\Theta = 0,\, B = 1$ towards $\Theta = q = \arccos 2/\pi,\, B = 1$ along the zero line $B = 1$. We omit the analogous considerations for $\Theta = -q$. By lemma 7.2 we encounter intersections at

$$\Theta = \Theta_{k+2m}^+ = \Theta(\Omega_{k+2m}^+)\,. \tag{9.9}$$

Since $0 < \Theta < q = \Theta(\Omega = 1)$ the values of $\Omega = \Omega_{k+2m}^+$ are restricted to $1 < \Omega < 2$. Here we have used that $\Theta(\Omega)$ is strictly decreasing; see proposition 7.1. This

identifies the $[\,k/2\,]$ intersections (9.9) to occur at positive $m = 1, 2, \ldots, [\,k/2\,]$; see (7.12) and (7.17).

By lemma 7.3 the Hopf curves intersect the zero line $B = 1$ transversely at $\Theta = \Theta^{\iota}_{k+2m}$. Since $m > 0$, $\iota = +$, the direction is towards increasing B and decreasing Θ in our case. Therefore the total unstable dimension $E = E(\Theta,\, B = 1)$ decreases by 2 as Θ increases through any of the $[\,k/2\,]$ crossing values $\Theta = \Theta^{+}_{k+2m}$, $m = 1, 2, \ldots, [\,k/2\,]$; see jump property (9.8) and the blue color coding in figs. 1.2, 4.1. Hence

$$E(\Theta = q,\, B = 1) = E(\Theta = 0,\, B = 1) - 2\,[\,k/2\,] = 0 \tag{9.10}$$

for any parity of k, if we insert (9.7). This proves claim (9.4) and the lemma. $\bowtie$

Lemma 9.2. *For $\varepsilon > 0$ small enough, the interior of the regions $\mathcal{P}^{\iota}$, $\iota = \pm$, defined by their boundary curves $B = 1$, Γ^0_k and $\Gamma^{\iota}_{k,\,\pm}$ does not contain points on any other Hopf curves.*

Proof. Our proof is indirect. We assume that there exists a subsequence $k \to \infty$, i.e. $\varepsilon = 1/\omega_k \to 0$, with associated solutions

$$\chi(\Omega_k,\, \Phi_k,\, \Theta_k,\, B_k) = 0 \tag{9.11}$$

of the scaled characteristic equation (4.5) with $(\Theta_k,\, B_k)$ in the interior of $\mathcal{P}^+$, say. By compactness of the region of interest $0 \le \Omega_k \le 2$, $|\Theta_k| \le 1$, and $-\pi/2 \le \Phi_k < 3\pi/2$ with $\Phi_k \in S^1$, we may assume convergence to a limiting solution

$$\chi(\Omega_*,\, \Phi_*,\, \Theta_*,\, B_*) = 0\,. \tag{9.12}$$

The definition of the region $\mathcal{P}^+$ implies

$$\Theta_* = q = \arccos\, 2/\pi \quad \text{and} \quad B_* = 1\,. \tag{9.13}$$

In case $\Omega_* > 0$, section 7 implies $\Phi_* = \Phi(\Omega_*)$, $\Theta_* = \Theta(\Omega_*)$ and $\Omega_* = 1$. In (7.5) of proposition 7.1 we have studied the limit $\Omega_k \to 1$ and in lemma 5.3 we have established uniform transversality of the Hopf curves to the zero line, in this limit. In particular the Hopf curves $m = \pm 1$ through $\Theta = \Theta^{\iota}_{k\pm 2}$ do not admit any other Hopf curves between them, in the limit $\Omega \to 1$. See also the resonance gap in hashing fig. 4.2 and lemma 5.3.

It remains to consider the Takens-Bogdanov limit $\Omega_k \to \Omega_* = 0$. In this limit we have the expansion (6.6), (6.7) of the spiraling Hopf curve which emanates from the Takens-Bogdanov point $\Theta_{\mathrm{TB}} = (-1)^{k+1}$, $B_{\mathrm{TB}} = 1$. In particular $\Theta_* = q = \arccos\, 2/\pi$ implies

$$\Phi_* = \arcsin\, q\,, \tag{9.14}$$

with $\mathrm{sign}\,(\Phi^* - \pi/2) = (-1)^{k+1}$. Since all further branches of the Hopf spiral possess larger distance $B - 1 = \beta\,\Omega$ from $B = 1$ than the first one Γ^0_k, of $0 \le \omega = \Phi - \Phi_{\mathrm{TB}} \le \pi$, which defines the boundary of $\mathcal{P}^+$, there cannot be any further Hopf curves in the interior of $\mathcal{P}^+$, for large enough k. This proves the lemma. $\bowtie$

Lemma 9.3. *The curves* $B = 1$, Γ^0_k, $\Gamma^\iota_{k,\pm}$ *transform to the curves* $b = b_k = (-1)^k 2/\omega_k$, γ^0_k, $\gamma^\iota_{k,\pm}$ *of theorem 1.1.*

The expansions (6.11), (6.12) *for* Γ^0_k *and* (5.2) – (5.4), (5.12), (7.19) *for* $\Gamma^\iota_{k,\pm}$ *imply the expansions* (1.11) – (1.16) *for the Pyragas regions* $\mathcal{P}^\iota_k$.

Proof. We aim for the precise symbolic expansions (1.11), (1.12), (1.14), (1.15); the numerical evaluations (1.13), (1.16) are trivial consequences. To pass from $B_* = 1$, Γ^0_k, $\Gamma^\iota_{k,\pm}$ to $b = b_k$, γ^0_k, $\gamma^\iota_{k,\pm}$ we only have to revert the scaling (4.3). In terms of (Θ, B) the claims (1.11), (1.12) read

$$B^\iota_k = 1 + (-1)^k \cdot \tfrac{1}{2}\, b^\iota_k\, \varepsilon + \dots \tag{9.15}$$

$$\Theta^\iota_{k,\pm} = \iota\, q \pm \Theta_{k+2}\, \varepsilon + \dots \tag{9.16}$$

with q, Θ_{k+2}, b^ι_k and the slopes σ^ι_k of the approximating parallelograms given by (1.14) – (1.15). Here expansions are only required up to errors of order ε^2.

By lemma 9.2, the value $B = B^\iota_k$ approximates B for Γ^0_k in the region $\mathcal{P}^\iota$, and $\Theta = \Theta^\iota_{k,\pm}$ approximates the intersection points of $\Gamma^\iota_{k,\pm}$ with the zero line $B = 1$. The slopes σ^ι_k are the slopes of $\Gamma^\iota_{k,\pm}$ at intersection.

In lemma 7.2, (7.15) we have identified $\Theta^\iota_{k,\pm} = \iota\, \Theta(\Omega^\iota_{k\pm2})$. Expansion (7.19) for $\Theta(\Omega^\iota_{k\pm2})$ on $\Gamma^\iota_{k,\pm}$ there implies (9.15) with q and Θ_{k+2} given by (1.14). This proves claim (9.16).

To prove claim (9.15) we invoke expansion (6.12) for the curve $\Gamma^0_k : \omega \mapsto (\Theta(\omega), B(\omega))$. Note $0 < \omega < \pi$ on Γ^0_k. On the boundary part Γ^0_k of $\mathcal{P}^\iota$ we have $\Theta = \iota\, q + \dots$, up to order ε. Therefore the Θ-expansion in (6.12) implies $\omega^\iota_k = \frac{\pi}{2} + (-1)^k\, \iota \arcsin q + \dots$ up to order ε. The B-expansion then asserts

$$B = 1 + (-1)^k\, \varepsilon\, \omega^\iota_k \sin\, \omega^\iota_k + \dots\,. \tag{9.17}$$

This implies (9.15) with

$$b^\iota_k = 2\omega^\iota_k \sin\, \omega^\iota_k = (\pi + 2\Phi^\iota_k) \cos\, \Phi^\iota_k\,, \tag{9.18}$$

if we substitute $\omega^\iota_k = \frac{\pi}{2} + \Phi^\iota_k$ as in (1.15).

It remains to determine the slopes $\sigma^\iota_k = db/d\vartheta = (-1)^k\, 2\, dB/d\Theta$ of the Hopf curves $\gamma^\iota_{k,\pm}$, alias $\Gamma^\iota_{k,\pm}$, at the crossings $\Theta = \Theta^\iota_{k,\pm}$ of the zero line $B = 1$; see (1.16). Since the sides of $\mathcal{P}^\iota$ have lengths of order ε^2 it is sufficient to determine the slopes σ^ι_k up to errors of order ε. Since the crossings at $\Theta = \Theta^\iota_{k,\pm}$ themselves are ε-close to $\Theta = \iota\, q$, we can invoke (7.29), (7.30) and the expansions (7.19) to conclude

$$\begin{aligned} \sigma^\iota_k &= 2\,(-1)^k \left.\frac{dB}{d\Theta}\right|_{\Theta=\iota q} + \dots = (-1)^{k+1}\pi\, \sin(\iota\, q) + \dots = \\ &= 2\,(-1)^{k+1}\iota \sqrt{(\tfrac{\pi}{2})^2 - 1} + \dots\,. \end{aligned} \tag{9.19}$$

Assertion (9.19) now proves claim (1.14) on σ, and completes the proof of the lemma and of theorem 1.2 alike. ⋈

10 Concluding remarks

Our analysis above has achieved noninvasive stabilization of periodic solutions near Hopf bifurcation of scalar pure delay equations. Stabilization was achieved by linear feedback control of Pyragas type

$$\dot{x}(t) = \lambda f\big(x(t-1)\big) + b^{-1}\big(x(t-\vartheta) + (-1)^{n+1}x(t-\vartheta-np/2)\big)\,, \tag{10.1}$$

with real control amplitude $1/b$, at the expense of introducing two more delays ϑ and $\vartheta + np/2$. Here $p > 0$ denoted the constant minimal period of the bifurcating periodic solutions. Oddness of the nonlinearity f and of the bifurcating periodic solutions enabled us to choose half-period delay $n = 1$ throughout the paper. With the normalization $f'(0) = 1$, we succeeded to stabilize any supercritical Hopf bifurcation at all parameters

$$\lambda = \lambda_k = (-1)^{k+1}\omega_k\,, \quad p = p_k = 2\pi/\omega_k\,, \quad \omega_k = (k+1/2)\pi\,; \tag{10.2}$$

see (1.6), (1.7) and theorems 1.1 and 1.2. In particular this demonstrates delayed feedback stabilization for any sufficiently large, even or odd unstable dimension $k \in \mathbb{N}_0$ of the periodic orbits by the single linear control scheme (10.1). There was no odd number limitation in our result. Differently from previous results [Fie&al07, Fie08, Bly&al08, Cho&al14], our result did not require any rotationally equivariant normal form of Stuart-Landau type, or any reduction to such normal forms as in [BrPoSi11]. The proper choices of feedback amplitudes $1/b$ and delay offsets ϑ, however, turned out to be a delicate matter, with only tiny Pyragas regions $\mathcal{P}^{\pm}$ of guaranteed success.

In this concluding section we comment on the case of small k which is ignored by our asymptotic analysis. Since we have not been able to detect, or even prove, further Pyragas regions in our setting, we then comment on the promising case $n = k$ of delays at multiples n of the half-period $p/2$. We conclude with a broader view of general delay equations and an open question on a more fundamental apparent Floquet limitation of Pyragas control.

For low values $k = 1, \ldots, 4$ we have sketched the resulting numerical Takens-Bogdanov spirals in fig. 10.1. For $k = 1$ the Pyragas region $E(\Theta, B) = 0$ is bounded by the red part of the dashed horizontal zero line $B = 1$, from above, and from below by the solid blue Hopf branch Γ_1^0 emanating from the solid black Takens-Bogdanov point. All stability claims can easily be verified from the color coding; see fig. 1.1 and the arguments in sections 8 and 9. The same horizontal boundaries apply for $k = 3$, but an additional vertical boundary $\Gamma_{k,+}^{\iota}$, $\iota = \pm$ has appeared from the top blue Hopf curve at $\Theta = 0$. This splits the Pyragas region $E(\Theta, B) = 0$ into two connected components $\mathcal{P}^{\pm}$ underneath the horizontal red dashed zero line $B = 1$. The first such splitting occurs, analogously, for $k = 2$ above the blue dashed zero line $B = 1$. The first case which features both additional boundaries $\Gamma_{k,\pm}^{\iota}$ of the Pyragas regions $\mathcal{P}^{\iota}$, $\iota = \pm$, is $k = 4$. This numerical

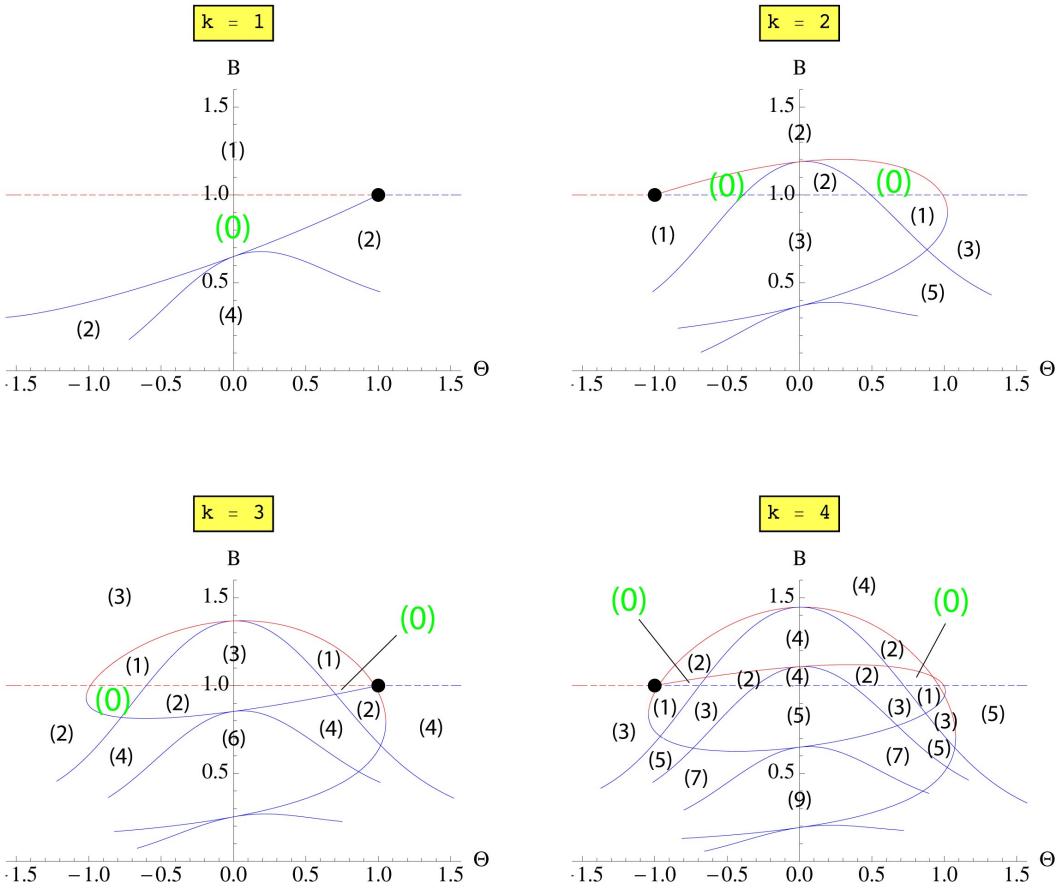

Figure 10.1: *Zooms of the Takens-Bogdanov spirals as in fig. 4.1 for low hashing values* $k = 1, \ldots, 4$. *Unstable dimensions* $E(\Theta, B)$ *are indicated in parentheses. The stabilized Pyragas regions* (0)*, in green, are described in the text.*

evidence supports our expectation that theorem 1.1 holds for all $k \geq 4$, and extends to the remaining cases $k = 1$, 2, 3 with the above minor modifications.

For delayed feedbacks of the form (10.1) we did not detect other Pyragas regions $E(\Theta, B) = 0$ at half-period delay $n = 1$, for any $k > 0$. The only other Pyragas regions which we did encounter occurred for $n = k$ at small values of $\vartheta > 0$ and $1/|b|$. Since these regions may be accessible to a two-scale analysis much in the spirit, if not the letter, of the present paper we plan to address them on another occasion.

For nonlinearities f which fail to be odd, an unresolved difficulty arises here. Since periodic solutions of the pure delay equation lose their odd-symmetry property (2.3), only even n are noninvasive. For odd k this puts Pyragas stabilization (10.1) in limbo.

Although we only addressed the pure delay equation $\dot{x}(t) = \lambda f(x(t-1))$ as our target of delayed feedback control (10.1), more general (odd) delayed systems

appear accessible. We mention

$$\dot{x} = f\big(\lambda,\, x(t),\, x(t-1)\big) \tag{10.3}$$

with scalar or vectorial x. For some numerical observations in such settings see [Bly&al08, Cho&al14] for example. The only reason of our preference for the pure delay equation was the ease of a coherent treatment of all Hopf bifurcations, in section 2. This put proper emphasis on the prerequisite linear analysis of characteristic equations.

Far from Hopf bifurcation such linear analysis at equilibria is not sufficient. Linear instability of periodic orbits is then regulated by Floquet exponents η or their associated Floquet multipliers $\mu = \exp(\eta p)$. In fact the mere study of Floquet theory itself is a demanding subject for delay equations; see [MPSe96a, WalSku02, SkuWal03, SkuWal05]. Only for rotating wave solutions in planar rotationally equivariant ODE systems have we been able to study Pyragas stabilization of periodic orbits with any mathematical rigor, so far. Much to our surprise we encountered a *Floquet limitation*

$$\eta < 9\,, \tag{10.4}$$

for the Floquet exponent η, beyond which it became impossible to stabilize the periodic orbit; see [Fie08]. This bound held, independently of the particular nonlinearity f, for nonlinear delayed feedback controls with delay off-set $\vartheta = 0$ and general complex controls b. Our analysis heavily relied on equivariance. In particular this allowed us to freeze the rotating wave by passing to co-rotating coordinates. Only then could the required Floquet analysis be reduced to a certain characteristic equation involving exponentials.

In our present example (10.1) Floquet exponents η of the bifurcating periodic solutions are inherited from the eigenvalues μ of the equilibrium $x = 0$ at bifurcation $\lambda = \lambda_k$. The real part of the most unstable μ grows like $\log k$ and violates the bound (10.4). Nevertheless our control scheme did succeed. The lowest unstable real part of μ, on the other hand, is of order $2/k$ and does not violate (10.4). This *dominant Floquet exponent* describes the exponential rate of generic convergence to the periodic solution in backwards time, on the unstable manifold. Whether or not a Floquet limitation for Pyragas control prevails in nonequivariant ODE settings (1.1), or even the simplest delay settings (10.3) and its pure delay variant (1.2), remains open for the dominant Floquet exponent.

References

[BeCo63] R. Bellman and K.L. Cooke. *Differential-Difference Equations*. Academic Press, New York, 1963.

[BiRo62] G. Birkhoff and G.-C. Rota. *Ordinary Differential Equations*. Ginn and Company, Boston, 1962.

[Bly&al08] K.B. Blyuss, Y.N. Kyrychko and E. Schöll. Control of unstable steady states in neutral time-delayed systems. Eur. Phys. J. B. **65** (2008) 571–576.

[BrPoSi11] G. Brown, C.M. Postlethwaite and M. Silber. Time-delayed feedback control of unstable periodic orbits near a subcritical Hopf bifurcation. Physica D. **240** (2011) 1–13.

[Cho&al14] C.-U. Choe, R.-S. Kim, H. Jang, P. Hövel and E. Schöll. Delayed-feedback control: arbitrary and distributed delay-time and noninvasive control of synchrony in networks with heterogeneous delays. Int. J. of Dynamics and Control. **2** (2014) 2–25.

[ChoLau00] P. Chossat and R. Lauterbach. *Methods in Equivariant Bifurcations and Dynamical Systems*. Advanced Series in Nonlinear Dynamics **15**, World Scientific, Singapore, 2000.

[Die&al95] O. Diekmann, S.A. van Gils, S.M. Verduyn-Lunel and H.-O. Walther. *Delay Equations: Functional-, Complex-, and Nonlinear Analysis*. App. Math. Sci. **110**, Springer-Verlag, New York, 1995.

[Dor89] P. Dormayer. Smooth bifurcation of symmetric periodic solutions of functional differential equations. J. Differ. Equations. **82** (1989) 109–155.

[Fie88] B. Fiedler. *Global Bifurcation of Periodic Solutions with Symmetry*. Lect. Notes Math. **1309**, Springer-Verlag, Heidelberg, 1988.

[Fie08] B. Fiedler. Time-delayed feedback control: qualitative promise and quantitative constraint. In *6th EUROMECH Conference on Nonlinear Dynamics ENOC 2008*. (A.L. Fradkov et al., eds.), Saint Petersburg, Russia, 2008.

[Fie&al07] B. Fiedler, V. Flunkert, M. Georgi, P. Hövel and E. Schöll. Refuting the odd number limitation of time-delayed feedback control. Phys. Rev. Lett. **98** (2007) 114101.

[Fie&al08] B. Fiedler, V. Flunkert, M. Georgi, P. Hövel and E. Schöll. Beyond the odd-number limitation of time-delayed feedback control. In *Handbook of Chaos Control*. (E. Schöll et al., eds.), Wiley-VCH, Weinheim, (2008) 73–84.

[Fie&al10] B. Fiedler, V. Flunkert, P. Hövel and E. Schöll. Delay stabilization of periodic orbits in coupled oscillator systems. Phil. Trans. Roy. Soc. A. **368** (2010) 319–341.

[FieMP89] B. Fiedler and J. Mallet-Paret. Connections between Morse sets for delay differential equations. J. Reine Angew. Math. **397** (1989) 23–41.

[GoStSch88] M. Golubitsky, I. Stewart and D. Schaeffer. *Singularities and Groups in Bifurcation Theory*. AMS 69 **2**, Springer-Verlag, New York, 1988.

[Hale77] J.K. Hale. *Theory of Functional Differential Equations*. Springer-Verlag, New York, 1977.

[HaleVL93] J.K. Hale and S.M. Verduyn-Lunel. *Introduction to Functional Differential Equations*. Springer-Verlag, New York, 1993.

[Har&al06] F. Hartung, T. Krisztin, H.-O. Walther and J. Wu. Functional differential equations with state-dependent delays: theory and applications. In *Handbook of Differential Equations: Ordinary Differential Equations, Vol. III.* (A. Cañada, P. Drábek and A. Fonda eds.), Elsevier/North-Holland, Amsterdam, (2006) 435–545.

[Ju&al07] W. Just, B. Fiedler, V. Flunkert, M. Georgi, P. Hövel and E. Schöll. Beyond the odd number limitation: A bifurcation analysis of time-delayed feedback control. Phys. Rev. E. **76** (2007) 026210.

[KapYor74] J.L. Kaplan and J.A. Yorke. Ordinary differential equations which yield periodic solutions of differential delay equations. J. Math. Analysis Appl. **48** (1974) 317–324.

[KolMysh99] V. Kolmanovski and A. Myshkis. *Introduction to the Theory and Applications of Functional Differential Equations*. Kluwer, Dordrecht, 1999.

[Kri08] T. Krisztin. Global dynamics of delay differential equations. Period. Math. Hung. **56** (2008) 83–95.

[KyBlSch08] Y.N. Kyrychko, K.B. Blyuss and E. Schöll. Control of unstable steady states in neutral time-delayed systems. Eur. Phys. J. B. **65** (2008) 571–576.

[KyBlSch11] Y.N. Kyrychko, K.B. Blyuss and E. Schöll. Amplitude death in systems of coupled oscillators with distributed-delay coupling. Eur. Phys. J. B. **84** (2011) 307–315.

[MP88] J. Mallet-Paret. Morse decompositions for differential delay equations. J. Differ. Equations. **72** (1988) 270–315.

[MPNu92] J. Mallet-Paret and R.D. Nussbaum. Boundary layer phenomena for differential-delay equations with state-dependent time-lags: I. Arch. Ration. Mech. Analysis **120** (1992) 99–146.

[MPNu96] J. Mallet-Paret and R.D. Nussbaum. Boundary layer phenomena for differential-delay equations with state-dependent time-lags: II. J. Reine Angew. Math. **477** (1996) 129–197.

[MPNu03] J. Mallet-Paret and R.D. Nussbaum. Boundary layer phenomena for differential-delay equations with state-dependent time-lags: III. J. Differ. Equations **189** (2003) 640–692.

[MPNu11] J. Mallet-Paret and R.D. Nussbaum. Stability of periodic solutions of state-dependent delay-differential equations. J. Differ. Equations. **250** (2011) 4085–4103.

[MPSe96a] J. Mallet-Paret and G. Sell. Systems of differential delay equations: Floquet multipliers and discrete Lyapunov functions. J. Differ. Equations **125** (1996) 385–440.

[MPSe96b] J. Mallet-Paret and G. Sell. The Poincaré–Bendixson theorem for monotone cyclic feedback systems with delay. J. Differ. Equations **125** (1996) 441–489.

[Nu78] R.G. Nussbaum. *Differential-Delay Equations with Two Time Lags.* Mem. Am. Math. Soc. **205**, Providence, RI, 1978.

[Nu02] R.G. Nussbaum. Functional differential equations. In *Handbook of Dynamical Systems, Vol. II.* (B. Fiedler ed.), Elsevier/North-Holland, Amsterdam, (2002) 461–499.

[Nak97] H. Nakajima. On analytical properties of delayed feedback control of chaos. Phys. Lett. A. **232** (1997) 207–210.

[NakUe98] H. Nakajima and Y. Ueda. Half-period delayed feedback control for dynamical systems with symmetries. Phys. Rev. E. **58** (1998) 1757–1763.

[PoSi07] C.M. Postlethwaite and M. Silber. Spatial and temporal feedback control of traveling wave solutions of the two-dimensional complex Ginzburg-Landau equation. Physica D. **236** (2007) 65–74.

[PoBrSi13] C.M. Postlethwaite, G. Brown and M. Silber. Feedback control of unstable periodic orbits in equivariant Hopf bifurcation problems. Phil. Trans. Roy Soc. A. **371** (2013) 20120467.

[Pyr92] K. Pyragas. Continuous control of chaos by self-controlling feedback. Phys. Lett. A. **170** (1992) 421–428.

[Pyr12] K. Pyragas. A twenty-year review of time-delay feedback control and recent developments. Int. Symp. Nonl. Th. Appl., Palma de Mallorca, 2012.

[Scha90] R. Schaaf. *Global Solution Branches of Two-Point Boundary Value Problems*. Springer-Verlag, New York, 1990.

[Schn13] I. Schneider. Delayed feedback control of three diffusively coupled Stuart-Landau oscillators: a case study in equivariant Hopf bifurcation. Phil. Trans. Roy. Soc. A. **371** (2013) 20120472.

[Schn14] I. Schneider. *Equivariant Pyragas Control*. Master Thesis, Freie Universität Berlin, 2014.

[SkuWal03] A.L. Skubachevskii and H.-O. Walther. On Floquet multipliers of slowly oscillating periodic solutions of nonlinear functional differential equations. Trans. Mosc. Math. Soc. **2003** (2003) 1–44.

[SkuWal05] A.L. Skubachevskii and H.-O. Walther. On the hyperbolicity of rapidly oscillating periodic solutions of functional differential equations. Funct. Analysis Appl. **39** (2005) 68–70.

[Wal95] H.-O. Walther. *The 2-Dimensional Attractor of* $\dot{x}(t) = -\mu x(t) + f(x(t-1))$. Mem. Amer. Math. Soc. **544**, Providence, RI, 1995.

[WalSku02] H.-O. Walther and A.L. Skubachevskii. On the spectrum of the monodromy operator for slowly oscillating periodic solutions to functional differential equations. Dokl. Math. **65** (2002) 382–385.

[Wri55] E.M. Wright. On a non-linear differential-difference equation. J. Reine Angew. Math. **194** (1955) 66–87.

[Wu96] J. Wu. *Theory and Applications of Partial Functional Differential Equations*. Springer-Verlag, New York, 1996.

[YuGuo14] J. Yu and Z. Guo. A survey on the periodic solutions to Kaplan-Yorke type delay differential equation-I. Ann. Differ. Equations. **30** (2014) 97–114.